No Tissue Damage by Chronic Deep Brain Stimulation in Parkinson's Disease

Christine Haberler, MD,* François Alesch, MD,†
Peter R. Mazal, MD,‡, Peter Pilz, MD,§
Kurt Jellinger, MD,‖ Michaela M. Pinter, MD,¶
Johannes A. Hainfellner, MD,* and Herbert Budka, MD*

We report on the pathological findings in the brains of 8 Parkinson's disease patients treated with deep brain stimulation (DBS) of the thalamic ventral intermediate nucleus (6 cases) and subthalamic nucleus (2 cases). DBS was performed continuously for up to 70 months. All brains showed well-preserved neural parenchyma and only mild gliosis around the lead track compatible with reactive changes due to surgical placement of the electrode. We conclude that chronic DBS does not cause damage to adjacent brain tissue.

Haberler C, Alesch F, Mazal PR, Pilz P, Jellinger K, Pinter MM, Hainfellner JA, Budka H. No tissue damage by chronic deep brain stimulation in Parkinson's disease. Ann Neurol 2000;48:372–376

In the 1950s and 1960s, thalamotomy was introduced as a treatment for tremor in Parkinson's disease (PD). It was empirically recognized that high-frequency stimulation (>100 Hz) of the thalamic ventral intermediate nucleus (VIM) produces tremor arrest. The discovery of L-dopa in 1967 replaced stereotactic surgery. In the 1980s, the side effects and limits of chronic L-dopa therapy became obvious and led to the reintroduction of surgical treatment of motor symptoms in PD. A new less destructive technique, deep brain stimulation (DBS), was developed.[1] During the last 10 years, several groups have demonstrated that chronic DBS of the VIM, subthalamic nucleus (STN), or internal globus pallidus is an effective treatment for disabling pharmacotherapy-resistant motor symptoms (tremor, rigor, bradykinesia) in PD (see review by Starr and co-workers[2]). Compared with ablative surgery, DBS is a less destructive and more adaptable method, that is, stimulus parameters can be changed to increase efficacy or reduce side effects. Although many patients have been successfully treated with DBS, little is known about the effects of long-term stimulation on adjacent brain tissue. So far, only one autopsy report on a PD patient stimulated discontinuously over 43 months is available.[3] Here, we report the neuropathological findings in 8 PD patients who had continuous DBS for up to 70 months. We show that chronic DBS does not cause damage to adjacent brain tissue.

From the *Institute of Neurology and Departments of †Neurosurgery and ‡Clinical Pathology, University of Vienna, ‖Ludwig Boltzmann Institute of Clinical Neurobiology, and ¶Neurological Hospital Maria-Theresien-Schlössel, Vienna, and the §Landesnervenklinik, Salzburg, Austria.

Received Dec 29, 1999, and in revised form Apr 13, 2000. Accepted for publication Apr 19, 2000.

Address correspondence to Prof H. Budka, Institute of Neurology, University of Vienna, AKH 04J, Währingergürtel 18-20, POB 48, A-1097 Wien, Austria.

Patients and Methods

The brains of 8 patients were investigated. The target site was the VIM in 6 patients and the STN in 2 patients. In 4 patients, bilateral stimulation was performed. None of the patients had a previous thalamotomy. Implantation of the leads was performed as described previously.[4] In brief, the implantation is performed under stereotactic conditions with local anesthesia using special computed tomography and magnetic resonance imaging scans as well as ventriculography. The target is first determined on a pure radioanatomical basis. The testing electrode is then inserted within the target area, and a neurophysiological examination is performed. Once the optimal point is localized, the permanent electrode is implanted. Quadripolar leads were implanted in 7 patients, and a monopolar lead was implanted in 1 patient (models SP5535, 3387 and 3389; Medtronic, Minneapolis, MN) Measurements of active contacts were 1.47 mm in diameter and 4 mm in length. After a screening phase of a few days up to 2 weeks, a pulse generator (ITREL; Medtronic) was connected to the lead and implanted subcutaneously in the infraclavicular area. Monopolar or bipolar stimulation was programmed using one or a combination of the four contacts. In Patients 1 through 7, stimulation was performed continuously. Patient 8 was stimulated irregularly for 2 days during a postoperative screening phase and thus served as a control to determine the acute changes after implantation. Stimulus parameters are listed in Table 1.

In all patients, the cause of death was unrelated to lead implantation or electrical stimulation (cardiovascular failure in Patients 2–4 and 6, myocardial infarction in Patients 1 and 8, anaplastic astrocytoma in Patient 5, and drowning in Patient 7).

Brains were immersion-fixed in 4% formalin. After 2 weeks of formalin fixation, leads were carefully removed and the brain was cut. Tissue blocks were sampled from different brain regions containing the lead track, lead tip, and area of the active electrodes. In Patients 6 and 7, an evaluation was performed on routinely processed archival paraffin blocks retrieved from two municipal Austrian neuropathology laboratories.

In Patients 1, 3, 6, 7, and 8, tissue blocks were cut perpendicular to the axis of the lead track, and in Patients 2, 4, and 5, slices were cut parallel to the axis of the lead track (Fig A and B). Tissue blocks were embedded in paraffin, and 4- to 8-μm sections were cut and stained. In serial sections, the tip of the lead was localized. The area of the active contact was then calculated, taking consideration of tissue

Table 1. Deep Brain Stimulation Parameters in 8 Parkinson's Disease Patients

	Case											
	1 le	2 le	2 ri	3 le	4 le	4 ri	5 ri	6 le	6 ri	7 le	7 ri	8 le
Target site	VIM	VIM	VIM	VIM	VIM	VIM	VIM	VIM	VIM	STN	STN	STN
Stimulation period (mo)	70	49	54	45	45	45	21	15	15	3	3	2 days
Voltage (amperes)												
V0	1.3	1.7	1.0	1.8	1.3	2.3	2.2	2.3	2.0	1.5	1.5	+
V1	2.8	2.9	3.8	4.4	1.0	1.3	3.5	3.6	3.1	2.5	2.0	+
Frequency (Hz)												
F0	130	130	130	130	130	130	130	130	130	130	130	+
F1	130	170	130	160	185	185	130	170	135	130	130	+
Pulse width (μsec)												
W0	60	90	60	60	90	120	60	60	60	60	60	+
W1	60	120	60	60	60	60	60	60	90	90	90	+
Δt (mo)	69.5	48.0	54.0	45.0	45.0	44.5	19.0	10.0	10.0	3.0	3.0	/

le = left cerebral hemisphere; ri = right cerebral hemisphere; VIM = thalamic ventral intermediate nucleus; STN = subthalamic nucleus; mo = months; V0, F0, W0 = postoperative setting of stimulus parameters; V1, F1, W1 = last setting of stimulus parameters before death; Δt = time difference between setting of stimulus parameters after operation and before death; + = different stimulus parameters were tested.

shrinkage due to fixation and paraffin embedding.[5] In areas adjacent to the active contact, a panel of conventional and immunocytochemical stains was performed on serial sections. The same stains were performed in areas around the insulated part of the lead in Patients 1 through 7. The distance between active contact and insulated parts of the leads ranged from 0.5 cm (Patient 3) to 4 cm (Patient 8). Conventional stains comprised hematoxylin and eosin, luxol fast blue (myelin sheaths), van Gieson (connective tissue), Bielschowsky silver impregnation (axons), and Kanzler methods (fibrillary astrogliosis). For immunolabeling, we used a polyclonal antibody against glial fibrillary acidic protein (Dako, Glostrup, Denmark) and monoclonal antibodies against neurofilament protein (Clone 2F11; Dako), synaptophysin (clone SY 38; Dako), and anti-human human leukocyte antigen DR to detect activated microglia (clone CR3/43; Dako). A Dako ChemMate detection kit was used as a secondary system.[6]

Results

DBS persistently improved tremor in Patients 1 through 6 (VIM target site) and rigidity and akinesia in Patient 7 (STN target site). The clinical details on Patient 7 have been published previously.[7] Patient 8, who was stimulated irregularly during the postoperative screening phase, showed clinical improvement that did not differ from a postoperative microthalamotomy effect observed in other patients. This is generally considered to be a sign of good placement of the lead. Voltage or frequency slightly increased in all patients over the clinical time course (see Table 1).

All brains displayed the morphological substrate of PD, including loss of pigmented neurons, Lewy bodies, and gliosis in the substantia nigra. Patient 5 showed a recurrent anaplastic astrocytoma of the right frontal and temporal region. In Patient 6, multiple bilateral small lacunar infarcts in the basal ganglia, congophilic angiopathy, and a nonrecent mass hemorrhage in the left occipital lobe were noted. Case 7 fulfilled the criteria for a neocortical stage of diffuse Lewy body disease according to the Newcastle criteria.[8] The exact anatomical localization of the active contacts is indicated in Table 2.

Irrespective of the duration of DBS, the histopathological findings in brain tissue adjacent to the active contact were similar in all cases, except for Patient 8, who died 2 days after electrode implantation. Tissue changes around the active contact and nonstimulated areas adjacent to the insulated parts of the lead did not differ (see Fig). Around the lead track, a thin inner capsule of connective tissue was noted. The thickness of this fibrous sheath ranged from 5 to 25 μm (see Table 2). There was no correlation between duration of stimulation and thickness of the fibrous sheath. A narrow rim of fibrillary gliosis (< 500 μm) abutted on the fibrous capsule (see Fig, C–E). In the adjacent brain tissue, a zone of less than 1 mm showed loosely scattered glial fibrillary acidic protein–positive reactive astrocytes. Gliosis was most pronounced in Patients 6 and 7, who were stimulated for 3 and 15 months, respectively, and also had slight microglial activation around the lead track (see Fig, O). In the track and adjacent tissue (<500 μm), scarce mononuclear leukocytes, siderophages, and single multinucleated giant cells were detectable. In Patient 7, a slight inflammatory reaction with multinucleated giant cells engulfing tiny fragments of foreign material was observed. Even close to the track, neurons were well preserved and synaptophysin-immunoreactive structures were present (see Fig, I and K). Quantification of neuronal content around the lead track was not performed because of variability in exact location, with resulting variability of adjacent gray matter. No loss of axons or myelin sheaths was detectable (see Fig, D and J). In Cases 2, 4, 5, 6, and 7, single axonal spheroids were noted. In Patient 8, who was stimulated only for 2 days, minor fresh hemorrhage, perifocal edema, and numerous ax-

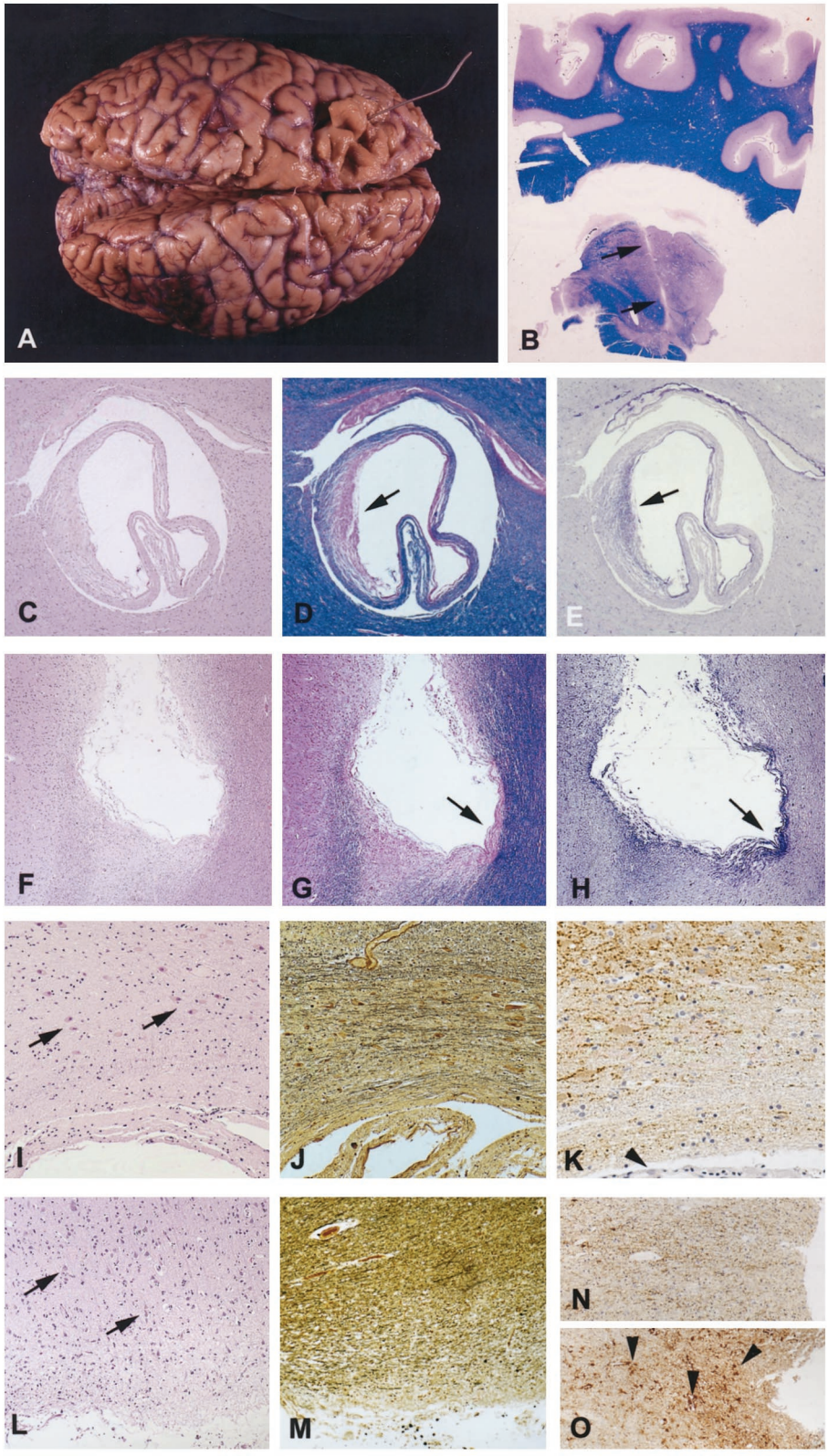
A
B
C
D
E
F
G
H
I
J
K
L
M
N
O

Table 2. Histopathology around the Lead Track in 8 Parkinson's Disease Patients Treated by Deep Brain Stimulation

	Case											
	1 le	2 le	2 ri	3 le	4 le	4 ri	5 ri	6 le	6 ri	7 le	7 ri	8 le
Target site	VIM	VIM	VIM	VIM	VIM	VIM	VIM	VIM	VIM	STN	STN	STN
Histological localization	VIM[a]	VIM(e)	VIM(e)	VIM(e)	VIM(e)	VIM[a]	VIM[a]	VIM(e)	VIM(e)	CI	STN	STN
Stimulation period	70 mo	49 mo	54 mo	45 mo	45 mo	45 mo	21 mo	15 mo	15 mo	3 mo	3 mo	2 days
Fibrous sheath (thickness in μm)	5	5	25	25	25	/[b]	8	5	13	5	5	/
Fibrillary gliosis < 500 μm	+	+	+	+	+	+	+	+	+	+	+	/
Reactive astrocytes < 1 mm	/	/	/	1	1	1	/	1	1	1	1	/
Multinucleated giant cells	/	/	/	/	1	1	1	1	1	2	2	/
Mononuclear leukocytes	1	1	2	1	1	/[b]	1	1	1	2	2	/
Macrophages	/	1	1	1	1	/[b]	1	1	1	1	2	/
Microglial activation	/	/	nd	/	nd	nd	nd	+	+	+	+	/
Axonal spheroids	/	1	1	/	1	/	1	2	2	1	1	3
Fresh hemorrhage	/	/	/	/	/	/	/	/	/	/	+	+
Perifocal edema	/	/	/	/	/	/	/	/	/	/	+	+

[a]Cutting plane of the histological section does not allow precise localization of the active contact.
[b]Some tissue was torn away when electrode was removed at autopsy.

le = left cerebral hemisphere; ri = right cerebral hemisphere; VIM(e) = thalamic ventral intermediate nucleus (externus); STN = subthalamic nucleus; CI = capsula interna immediately to STN; mo = months; + = present; nd = not done (too little material available); / = absent; 1 = single; 2 = some; 3 = numerous.

onal spheroids were found, representing acute changes after implantation. Details of the histopathological findings are listed in Table 2.

Discussion

Although DBS is a well-established treatment for PD, little is known about effects of chronic DBS on brain tissue. Some concern exists with regard to the potential risk of chemical changes like water electrolysis to H_2 and O_2 and the possibility of scarring around the lead with subsequent decrease of stimulation efficacy. Morphological analysis of stimulated tissues is thus needed. Experimental studies in cats[9–12] and monkeys[13] revealed only minor brain tissue damage, including fibrillary gliosis and mild lesioning of the neural parenchyma. Animals were stimulated only at irregular short intervals, maximum stimulation periods lasted only up to 18 months, and potential interspecies differences should be considered, however.

Studies with stimulus parameters similar to those used in our patients were performed in chronic pain patients[14–17] and 1 PD patient.[3] In some of these patients, stainless steel was used as lead material; however, it does not seem to have the same degree of biocompatibility as the platinum-iridium used in our leads. The chronic pain patients were stimulated for up to 20 months, and the PD patient was stimulated for 43 months. All these patients, however, were stimulated at irregular intervals,[14–17] or DBS was stopped at night.[3] The histopathological findings in these cases showed mild gliosis and minor neural damage around the lead track[3,15–17] or no damage at all.[14]

We present for the first time data in a series of PD patients stimulated continuously, including 1 patient with the longest stimulation period to date of 70 months. Comparison between shorter and longer periods of tissue stimulation did not reveal any progression of histopathological changes. We found no differences in stimulated and nonstimulated tissues adjacent to the lead track. There were only minor changes compatible with posttraumatic tissue reaction to the placement of the lead. Clinical long-lasting benefit correlates with the absence of progressive gliotic scar formation. A slight increase in stimulus parameters was necessary during the subsequent clinical course. This most likely resulted from the cessation of an initial microthalamotomy-like effect by the surgical trauma after 3 months and later from the progression of PD.

Fig. (A) External surface of a Parkinson's disease (PD) brain (Case 3) showing entry of a lead in the left frontal lobe. (B) Parasagittal section of cerebral hemisphere and thalamus (Case 2) showing the lead track (arrows). *PD Case 1. Histology of cross-cut lead track in the area of the active contact (C–E, I–K, N) and in a nonstimulated area 4 cm distant from the active contact (F–H, L, M). Myelin sheaths are mostly well preserved (D, G). There is only a small zone of myelin loss* (arrows *in D and G*), *which corresponds to fibrillary gliosis* (arrows *in E and H*). *Close to the active contact, neuronal cell bodies* (arrows *in I*) *and axons (dark fibers in J) are well preserved, and synaptophysin-positive structures (fine brown granular reaction product in K) are present. The arrowhead in K shows the thin fibrous capsule of the lead track. Distant from the active contact (L, M), changes do not differ from those around the active contact (I, J). In Case 1 (stimulation for 70 months), reactive gliosis is not present (N), whereas Case 7 (stimulation for 3 months) shows mild reactive astrogliosis around the active contact* (arrowheads *in O*). *(C, F: hematoxylin-eosin stain, ×30; I, L: hematoxylin-eosin stain, ×150; D, G: luxol fast blue stain, ×30; E, H: Kanzler stain, ×30; J, M: Bielschowsky silver impregnation, ×150; K: synaptophysin, ×150; N, O: glial fibrillary acidic protein, ×150).*

We conclude that chronic DBS does not cause damage to adjacent brain parenchyma.

We thank Helga Katz for excellent technical assistance, Dr Manfred Schmidbauer for kindly providing archival blocks of Case 6, and Dr Marin Guentchev for help and support.

References

1. Benabid AL, Pollak P, Louveau A, et al. Combined (thalamotomy and stimulation) stereotactic surgery of the VIM thalamic nucleus for bilateral Parkinson disease. Appl Neurophysiol 1987;50:344–346
2. Starr PA, Vitek JL, Bakay RA. Ablative surgery and deep brain stimulation for Parkinson's disease. Neurosurgery 1998;43: 989–1013
3. Caparros-Lefebvre D, Ruchoux MM, Blond S, et al. Long-term thalamic stimulation in Parkinson's disease: postmortem anatomoclinical study. Neurology 1994;44:1856–1860
4. Alesch F, Pinter MM, Helscher RJ, et al. Stimulation of the ventral intermediate thalamic nucleus in tremor dominated Parkinson's disease and essential tremor. Acta Neurochir (Wien) 1995;136:75–81
5. Böck P. Fixierung histologischer präparate. Romeis mikroskopische technik. 17th ed. München: Urban und Schwarzenberg, 1989
6. Guentchev M, Wanschitz J, Voigtlander T, et al. Selective neuronal vulnerability in human prion diseases: fatal familial insomnia differs from other types of prion diseases. Am J Pathol 1999;155:1453–1457
7. Pinter MM, Alesch F, Murg M, et al. Deep brain stimulation of the subthalamic nucleus for control of extrapyramidal features in advanced idiopathic Parkinson's disease: one year follow-up. J Neural Transm 1999;106:693–709
8. McKeith IG, Galasko D, Kosaka K, et al. Consensus guidelines for the clinical and pathologic diagnosis of dementia with Lewy bodies (DLB): report of the consortium on DLB international workshop. Neurology 1996;47:1113–1124
9. Woodford BJ, Carter RR, McCreery D, et al. Histopathologic and physiologic effects of chronic implantation of microelectrodes in sacral spinal cord of the cat. J Neuropathol Exp Neurol 1996;55:982–991
10. Mortimer JT, Shealy CN, Wheeler C. Experimental nondestructive electrical stimulation of the brain and spinal cord. J Neurosurg 1970;32:553–559
11. Stock G, Sturm V, Schmitt HP, Schlor KH. The influence of chronic deep brain stimulation on excitability and morphology of the stimulated tissue. Acta Neurochir (Wien) 1979;47:123–129
12. Yuen TG, Agnew WF, Bullara LA, et al. Histological evaluation of neural damage from electrical stimulation: considerations for the selection of parameters for clinical application. Neurosurgery 1981;9:292–299
13. Brown WJ, Babb TL, Soper HV, et al. Tissue reactions to long-term electrical stimulation of the cerebellum in monkeys. J Neurosurg 1977;47:366–379
14. Baskin DS, Mehler WR, Hosobuchi Y, et al. Autopsy analysis of the safety, efficacy and cartography of electrical stimulation of the central gray in humans. Brain Res 1986;371:231–236
15. Boivie J, Meyerson BA. A correlative anatomical and clinical study of pain suppression by deep brain stimulation. Pain 1982; 13:113–126
16. Gybels J, Dom R, Cosyns P. Electrical stimulation of the central gray for pain relief in human: autopsy data. Acta Neurochir Suppl (Wien) 1980;30:259–268
17. Kuroda R, Nakatani J, Yamada Y, et al. Location of a DBS-electrode in lateral thalamus for deafferentation pain. An autopsy case report. Acta Neurochir Suppl (Wien) 1991;52:140–142

Familial Alzheimer's Disease: Site of Mutation Influences Clinical Phenotype

C. F. Lippa, MD,* J. M. Swearer, PhD,†
K. J. Kane, MA,† D. Nochlin, MD,‡ T. D. Bird, MD,§
B. Ghetti, MD,‖ L. E. Nee, MSW,
P. St. George-Hyslop, MD, PhD,# D. A. Pollen, MD,†
and D. A. Drachman, MD†

Alzheimer's disease (AD) is caused by multiple genetic and/or environmental etiologies. Because differences in the genetically determined pathogenesis may cause differences in the phenotype, we examined age at onset and age at death in 90 subjects with dominantly inherited AD due to different mutations (amyloid precursor protein, presenilin-1, and presenilin-2 genes). We found that among patients with dominantly inherited AD, genetic factors influence both age at onset and age at death.

Lippa CF, Swearer JM, Kane KJ, Nochlin D, Bird TD, Ghetti B, Nee LE, St. George-Hyslop P, Pollen DA, Drachman DA. Familial Alzheimer's disease: site of mutation influences clinical phenotype. Ann Neurol 2000;48:376–379

Most cases of Alzheimer's disease (AD) are sporadic or nondominant; however, the discovery of genetic mutations in three different genes indicates that autosomal dominant AD is also an important cause of this disease.[1] Cases of AD with dominant transmission are due to mutations in the amyloid precursor protein (APP), presenilin (PS)-1 (PS-1), and PS-2 genes.[2–4] Mutations

From the *Department of Neurology, Medical College of Pennsylvania-Hahnemann University, Philadelphia, PA; †Department of Neurology, University of Massachusetts Medical School, Worcester, MA; ‡Department of Pathology, University of Washington School of Medicine, and §Department of Neurology, Veterans Affairs Medical Center and University of Washington School of Medicine, Seattle, WA; ‖Department of Pathology, Indiana University Medical Center, Indianapolis, IN; Family Studies Unit, National Institute of Neurological Disorders and Stroke, Bethesda, MD; and #Department of Medicine (Neurology) and Medical Biophysics, University of Toronto, Toronto, Ontario, Canada.

Received Apr 13, 2000. Accepted for publication Apr 21, 2000.

Address correspondence to Dr Swearer, Department of Neurology, University of Massachusetts Medical School, 55 Lake Avenue North, Worcester, MA 01655.

of the PS-1 gene on chromosome 14[5] are the most common abnormalities identified. Because numerous familial AD (FAD) kindreds lack mutations of the APP and PS-1 and PS-2 exons, it is possible that intronic mutations of these genes or unidentified genetic abnormalities exist that lead to autosomal dominant AD.

Despite its heterogeneous nature, all cases of AD have similar pathological characteristics, with β-amyloid plaques, intraneuronal neurofibrillary tangles, and neuronal loss as the hallmarks of the disease. Clinical, histopathological, and biochemical phenotypic heterogeneity has been described in AD groups as caused by either genetic etiologies or unknown etiologies, suggesting that the underlying disease process may not be identical when etiologies are different. Clinical and histopathological studies show subtle differences in features among AD groups.[1] For example, age at onset ("onset") and age at death ("death") may be earlier in PS-1 and APP AD than in sporadic AD. Reports of disease onset in specific kindreds show that affected members of PS-1 kindreds often develop symptoms in their fourth decade of life, APP kindreds in their fifth decade, and sporadic AD patients usually after the age of 60 years.[6] Even within PS-1 AD groups, onset varies from kindred to kindred, and there may be subtle age-related trends in onset depending on the site of the genetic defect within the PS-1 gene. Of the eight transmembrane (TM) domains in the PS-1 gene, kindreds with mutations of PS-1 TM loop 2 (TM2), TM3, TM7, and the loop connecting TM1 and TM2 have been reported to show extremely early onset.[7] Most studies of FAD kindreds have compared specific kindreds with sporadic AD, however. There are few formal studies comparing onset and death between groups of FAD subjects. We studied onset and death in 90 subjects with FAD due to different genetic etiologies.

Materials and Methods

Patients

We obtained brain tissue from 90 subjects with autosomal dominant FAD. There were 60 dementia subjects with confirmed mutations of the PS-1 gene. This group contained cases with mutations leading to alterations in the TM2 (n = 19), TM4 (n = 9), TM5 (n = 2), TM6 (n = 21), and TM8 (n = 9) portions of the expressed protein. Seventeen subjects with dementia had the same point mutation (N141I) of the PS-2 gene. Thirteen subjects with dementia had mutations of codon 717 of the APP protein. All 90 subjects met clinical criteria for probable AD[8] and showed histopathological features diagnostic of AD according to National Institute on Aging and Reagan Institute criteria.[9]

The subjects were all members of well-described FAD kindreds. Each subject was evaluated antemortem by a team associated with one of the authors. We assessed onset and death using review of medical records. Onset was estimated from the duration of symptoms as determined at the time of initial presentation.

Statistical Analyses

ANOVA was used to compare the PS-1, PS-2, and APP AD groups with regard to onset and death. A critical probability value less than 0.01 was adopted to partially correct for multiple comparisons. Significant differences were further analyzed using Tukey's honestly significant difference (HSD) test for multiple comparisons.

Results

Comparison of PS-1, PS-2, and APP AD Groups

AGE AT ONSET. A significant difference in onset was observed between groups ($p < 0.001$; Fig). Post hoc analyses of onset showed significant differences between the PS-2 group and both of the other 2 FAD groups ($p < 0.01$). Onset occurred a mean of 14.6 and 9.7 years earlier in the PS-1 and APP AD groups, respectively, than in the PS-2 AD group (Table 1).

AGE AT DEATH. A significant difference was found between the groups on age at death ($p < 0.001$; see Fig). Death occurred a mean of 16.2 years later in the PS-2 AD group than in the PS-1 AD group ($p < 0.01$; see Table 1). Death occurred a mean of 8.7 years later in the PS-2 group than in the APP group, but this did not reach a statistically significant level in the post hoc analysis ($p = 0.02$). Onset and death did not differ significantly between the APP and PS-1 groups.

Comparison of PS-1 Group by TM Domain versus PS-2 and APP

AGE AT ONSET. When the PS-1 group was subdivided by TM domain, overall significant differences in onset were found between the PS-2, APP AD, and PS-1 TM groups ($p < 0.001$). It was determined that the differences between the PS-1 AD and PS-2 AD groups were related to differences in specific PS-1 TM domains (Table 2). In PS-2 subjects, onset occurred later than that in PS-1 TM2, TM4, and TM6 AD subjects ($p < 0.01$ for post hoc comparisons). Onset did not differ significantly between the PS-2 group and the PS-1 TM8 group ($p = 0.02$).

Fig. Age at onset and age at death in presenilin (PS)-1 (PS-1), PS-2, and amyloid precursor protein Alzheimer's disease.

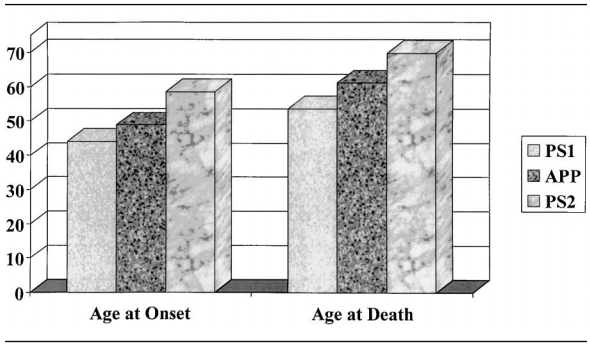

Table 1. Age at Onset and Age at Death in Presenilin-1, Presenilin-2, and Amyloid Precursor Protein Gene Mutations[a]

Gene	Onset[b] (range)	Death[c] (range)
Presenilin-1 (n = 60)	44.1 ± 7.8 (30–69)	53.7 ± 9.3 (37–81)
Presenilin-2 (n = 17)	58.6 ± 7.0 (45–73)	69.9 ± 7.6 (54–80)
Amyloid precursor protein (n = 13)	48.9 ± 6.7 (39–59)	61.2 ± 7.2 (46–72)

[a]Mean ± SD (range) in years.
[b]Onset: $F = 25.1$, $p < 0.001$; Tukey HSD: presenilin-2 > presenilin-1, amyloid precursor protein, $p < 0.01$.
[c]Death: $F = 24.0$, $p < 0.001$; Tukey HSD: presenilin-2 > presenilin-1, $p < 0.01$.

Table 2. Age at Onset and Age at Death by Transmembrane Domain[a]

Gene/Transmembrane Domain	Onset[b] (range)	Death[c] (range)
Presenilin-1		
Transmembrane loop 2 (n = 19)	41.3 ± 9.1 (30–69)	49.7 ± 9.4 (37–77)
Transmembrane loop 4 (n = 9)	40.2 ± 5.3 (30–48)	47.1 ± 5.1 (39–55)
Transmembrane loop 6 (n = 21)	46.3 ± 6.1 (36–57)	58.0 ± 6.8 (42–70)
Transmembrane loop 8 (n = 9)	49.0 ± 5.6 (42–57)	58.3 ± 10.4 (47–81)
Presenilin-2 (n = 17)	58.6 ± 7.0 (45–73)	69.6 ± 7.6 (54–80)
Amyloid precursor protein (n = 13)	48.9 ± 6.7 (39–59)	61.2 ± 7.2 (46–72)

[a]Mean ± SD (range) in years.
[b]Onset: F = 13.6, $p < 0.001$; Tukey HSD: presenilin-2 > presenilin-1 transmembrane loops 2, 4, 6, $p < 0.01$.
[c]Death: F = 15.7, $p < 0.001$; Tukey HSD: presenilin-2 > presenilin-1 transmembrane loops 2, 4, 6, $p < 0.01$; amyloid precursor protein > presenilin-1 transmembrane loops 2, 4, $p < 0.01$.

AGE AT DEATH. Significant differences between the groups were also found with regard to death ($p < 0.001$). Death was later in the PS-2 AD group than in the PS-1 TM2, TM4, and TM6 AD groups ($p < 0.01$ for post hoc comparisons; see Table 2). Death did not differ significantly between the PS-2 group and the TM8 group. Again, APP AD subjects had a later death than PS-1 TM2 and TM4 AD subjects ($p < 0.01$ for post hoc comparisons).

Apolipoprotein E Genotype

Information regarding apolipoprotein E (ApoE) genotype was available in 61 of the 90 cases. Twenty-eight percent of the subjects had at least one ApoE epsilon 4 allele, and 72% did not. ApoE epsilon 4 distribution in this sample had no effect on onset ($t = 0.2$, $p = 0.67$) or death ($t = 0.01$, $p = 0.94$). Too few subjects had an ApoE epsilon 2 allele to test for any epistatic effect[10] in our APP cases.

Discussion

Onset and death clearly differed between the PS-1, PS-2, and APP AD groups, although differences were present depending on the site of mutation, and there was variability within each group. In general, onset and death were later in the PS-2 AD group than in the PS-1 or APP AD group. We also noted differences in onset and death related to the site of the PS-1 mutation, with the TM2, TM4, and TM6 groups accounting for the differences between the PS-1 and PS-2 groups.

Despite these trends, patients within the same kindred or different kindreds linking to the identical TM region showed variation in onset and death, and subjects with mutations adjacent to one another sometimes showed differences in onset and death. This variability would suggest that factors determining onset and death also depend on other genetic factors or environmental modifiers. It is also possible that structurally conservative mutations result in later onset and death than mutations that lead to major conformational changes in the expressed gene. Although the presence and number of ApoE epsilon 4 alleles has been found to affect onset in late onset AD,[11] we found no association between ApoE genotype and onset in our early onset FAD groups. The results from this study demonstrate that onset and death vary in FAD cases depending on the specic sites of mutation.

This study was supported by NIH grant AG13623 (C.F.L.); NIH grant AG05134, the Stanley and Harriett Friedman Fund, and the Sterling Morton Research Trust (J.M.S., D.A.P., D.A.D., K.J.K.); NIH grants AG05136 and AG06781 (D.N.); and NIH grant AG05136 and Veterans Affairs Medical Research Funds (T.D.B.).

References

1. Lippa CF. Familial Alzheimer's disease: genetic influences on the disease process. Int J Mol Med 1999;4:529–536
2. Goate A, Chartier-Harlin M, Mullan M, et al. Segregation of a missense mutation of the amyloid precursor protein gene with familial Alzheimer's disease. Nature 1991;349:704–706
3. Levy-Lahad E, Wijsman EM, Nemens E, et al. A familial Alzheimer's disease locus on 18.chromosome 1. Science 1995;269: 970–973
4. Rogaev EI, Sherrington R, Rogaeva EA, et al. Familial Alzheimer's disease in kindreds with missense mutations in a gene on chromosome 1 related to the Alzheimer's disease type 3 gene. Nature 1995;376:775–778
5. St. George-Hyslop P, Haines J, Rogaev E, et al. Genetic evidence for a novel familial Alzheimer's disease locus on chromosome 14. Nat Genet 1992;2:330–334
6. Mullan M, Houlden H, Crawford F, et al. Age of onset in

familial early onset Alzheimer's disease correlates with genetic aetiology. Am J Med Genet 1993;48:129–130
7. Wegiel J, Wisniewski HM, Kuchna I, et al. Cell-type–specific enhancement of amyloid-beta deposition in a novel presenilin-1 mutation (P117L). J Neuropathol Exp Neurol 1998;57:831–838
8. McKhann G, Drachman DA, Folstein M, et al. Clinical diagnosis of Alzheimer's disease: report of the NINCDS-ADRDA Work Group under the auspices of Department of Health and Human Services Task Force on Alzheimer's Disease. Neurology 1984;34:939–944
9. National Institute on Aging, and Reagan Institute Working Group on Diagnostic Criteria for the Neuropathological Assessment of Alzheimer's Disease. Consensus recommendations for the postmortem diagnosis of Alzheimer's disease. Neurobiol Aging 1997;18(Suppl):S1–S2
10. Sorbi S, Nacimias B, Forleo P, et al. Epistatic effect of APP 717: mutation and apolipoprotein E genotype in familial Alzheimer's disease. Ann Neurol 1995;38:124–127
11. Corder EH, Saunders AM, Strittmatter WJ, et al. Gene dose of apolipoprotein E type 4 allele and the risk of Alzheimer's disease in late onset families. Science 1993;261:921–923

Severe Congenital Myasthenic Syndrome due to Homozygosity of the 1293insG ε-Acetylcholine Receptor Subunit Mutation

J. P. Sieb, MD,*¶ S. Kraner, MS,*† B. Schrank, MD,‡ B. Reitter, MD,§ T. H. H. Goebel, MD,‖ S. J. Tzartos, PhD,# and O. K. Steinlein, MD†

Recently, a congenital myasthenic syndrome (CMS) with end-plate acetylcholine receptor (AChR) deficiency due to missense mutations in the genes for the AChR subunit was described. The first observed patient with this CMS was heteroallelic for the two ε-AChR subunit mutations ε1101insT and ε1293insG. This patient had only a moderate phenotype with mild muscle weakness and abnormal fatigue. We have now found homozygosity for the ε1293insG mutation in a severely affected CMS patient, who lost the ability to walk in midchildhood and shows profound weakness and muscle wasting. Our observation allows a genotype-phenotype correlation illustrating how differences in the AChR mutation haplotype can profoundly influence disease severity.

Sieb JP, Kraner S, Schrank B, Reitter B, Goebel THH, Tzartos SJ, Steinlein OK. Severe congenital myasthenic syndrome due to homozygosity of the 1293insG (ε-acetylcholine receptor subunit mutation. Ann Neurol 2000;48:379–383

Congenital myasthenic syndromes (CMS) arise from presynaptic, synaptic, or postsynaptic defects of neuromuscular transmission. Mutations in the acetylcholine receptor (AChR) subunit genes are a common cause of postsynaptic CMS. They cause myasthenic weakness by changing the response of the AChR ion channel to acetylcholine or resulting in end-plate AChR deficiency.[1] CMS with end-plate AChR deficiency due to missense mutations in the AChR subunit genes was first described by Engel and co-workers.[2] These authors identified a 55-year-old myasthenic woman carrying two different frame-shifting ε-AChR subunit gene (CHRNE) mutations. In the heteroallelic state, these CHRNE mutations resulted in only mild muscular weakness and abnormal fatigue. We report on a patient homozygous for the more severe of the two mutations previously described by Engel and co-workers.[2] These differences in the AChR subunit mutation haplotype correlate phenotypic disease severity with genotypic changes.

Materials and Methods

All studies were approved by the Ethics Committee of the University Hospital Bonn, Germany, and informed consent was obtained from all individuals included in the study.

Muscle Biopsy

Muscle specimens were obtained from the gastrocnemius and quadriceps muscles at the ages of 9 and 19 years, respectively, and were analyzed as previously described.[3] For demonstration of the AChR with tetramethyl-rhodamine–labeled α-bungarotoxin (Molecular Probes, Eugene, OR), 5-μm cryostat sections were used. The tetramethyl-rhodamine–labeled α-bungarotoxin stains were combined with two-color immunofluorescence for laminin β2 (gift from U. Wewer, Copenhagen, Denmark) for localizing end plates. The γ-subunit of the AChR was localized in cryostat sections with two-color immunofluorescence by consecutive application of fluorescein-labeled α-bungarotoxin, anti-AChR γ-subunit (Mab66),[4] and rhodamine red-conjugated mouse anti-rat IgG (Jackson Laboratories, West Grove, PA). The Mab168 antibody[5] was used for detection of the ε-subunit of the AChR. All stains were compared with those at end plates of nonweak control subjects.

From the Departments of *Neurology and †Human Genetics, University of Bonn, Bonn; ‡Deutsche Klinik für Diagnostik, Wiesbaden; Departments of §Pediatrics and ‖Neuropathology, University of Mainz, Mainz; and ¶Max-Planck-Institute of Psychiatry, Munich, Germany; and #Department of Biochemistry, Hellenic Pasteur Institute, Athens, Greece.

Received Feb 8, 2000, and in revised form Apr 13. Accepted for publication Apr 14, 2000.

Address correspondence to Dr Steinlein, Institute for Human Genetics, University of Bonn, Wilhelmst 31, Bonn D-53105, Germany.

For additional immunohistochemical studies, the following antibodies were used: (1) dystrophin (Dys 1,2,3; Novocastra, Newcastle upon Tyne, UK); (2) merosin 80 (Chemicon, Temecula, CA) and 300 (Novocastra); (3) β-dystroglycan (Novocastra); (4) the sarcoglycans α (Novocastra), β (Novocastra), γ (Novocastra), and δ (gift from V. Nigro, Naples, Italy); (5) emerin (Novocastra); (6) spectrin (Novocastra); (7) caveolin (Dako, Hamburg, Germany); (8) utrophin, n-terminus (Novocastra); (9) developmental myosin (Novocastra); (10) vimentin (Dako); and (11) neural cell adhesive molecules (N-CAM; Dako). For detection of the primary antibodies, the avidin-biotinylated peroxidase technique (Vectastain ABC kit; Vector, Burlingame, CA) was used.

Genetic Studies

Single-strand confirmation analysis (SSCA) and heteroduplex analysis were used to screen for mutations in the CHRNE gene. The genomic sequences were obtained from the database sequence of clone hRPK.177_H_5mapl7 (accession number AC005973). Polymerase chain reaction and SSCA-heteroduplex analysis were performed using standard protocols. Direct sequencing of polymerase chain reaction products was performed on an ABI 377 sequencer using the BigDye Terminator Cycle Sequencing Ready Reaction kit (Applied Biosystems, Foster City, CA).

Results

Clinical Data

The patient is a 20-year-old woman from a consanguineous Moroccan marriage (Fig 1). Her parents and 7 living siblings are healthy. Two siblings died during early childhood because of severe respiratory infections. This patient started walking at the age of 13 months. After 2 years of age, the strength of her limb muscles

Fig 1. Pedigree of the family. The arrow indicates the propositus, who is homozygous for the mutation ε1293insG. Two siblings died during early childhood because of respiratory infections. Open symbols = unaffected, genotype not determined; half-filled symbols = unaffected, heterozygous for the mutation ε1293insG; cross symbol = unaffected, homozygous for the wild-type ε-subunit. Triangles indicate stillbirths.

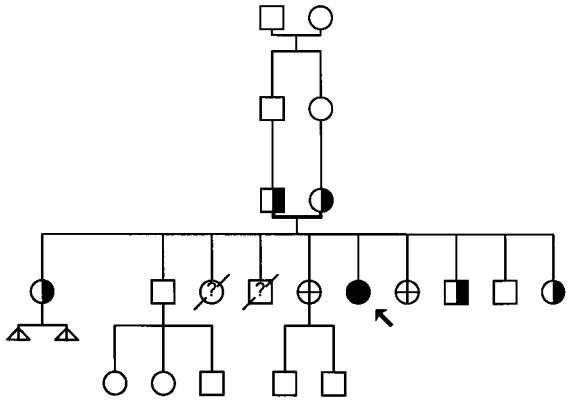

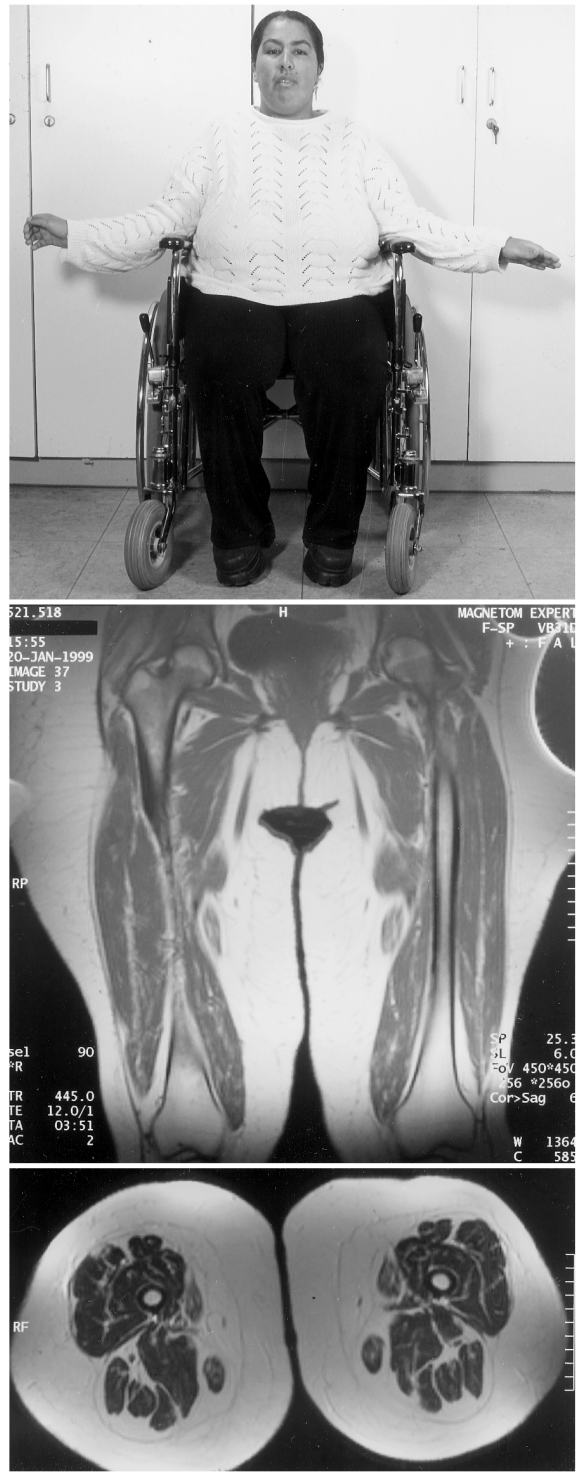

Fig 2. (Top) The propositus at the age of 20 years. Due to severe proximal muscle weakness, arm elevation is highly restricted, and she is permanently bound to the wheelchair. (Bottom) MRI of her thighs reveals severe muscle wasting. Excess fatty tissue is interspersed between the outer fascia and the remaining muscle tissue. This pattern of fatty replacement is distinctly unusual and not seen in other muscle diseases associated with fatty replacement of muscle such as the muscular dystrophies.

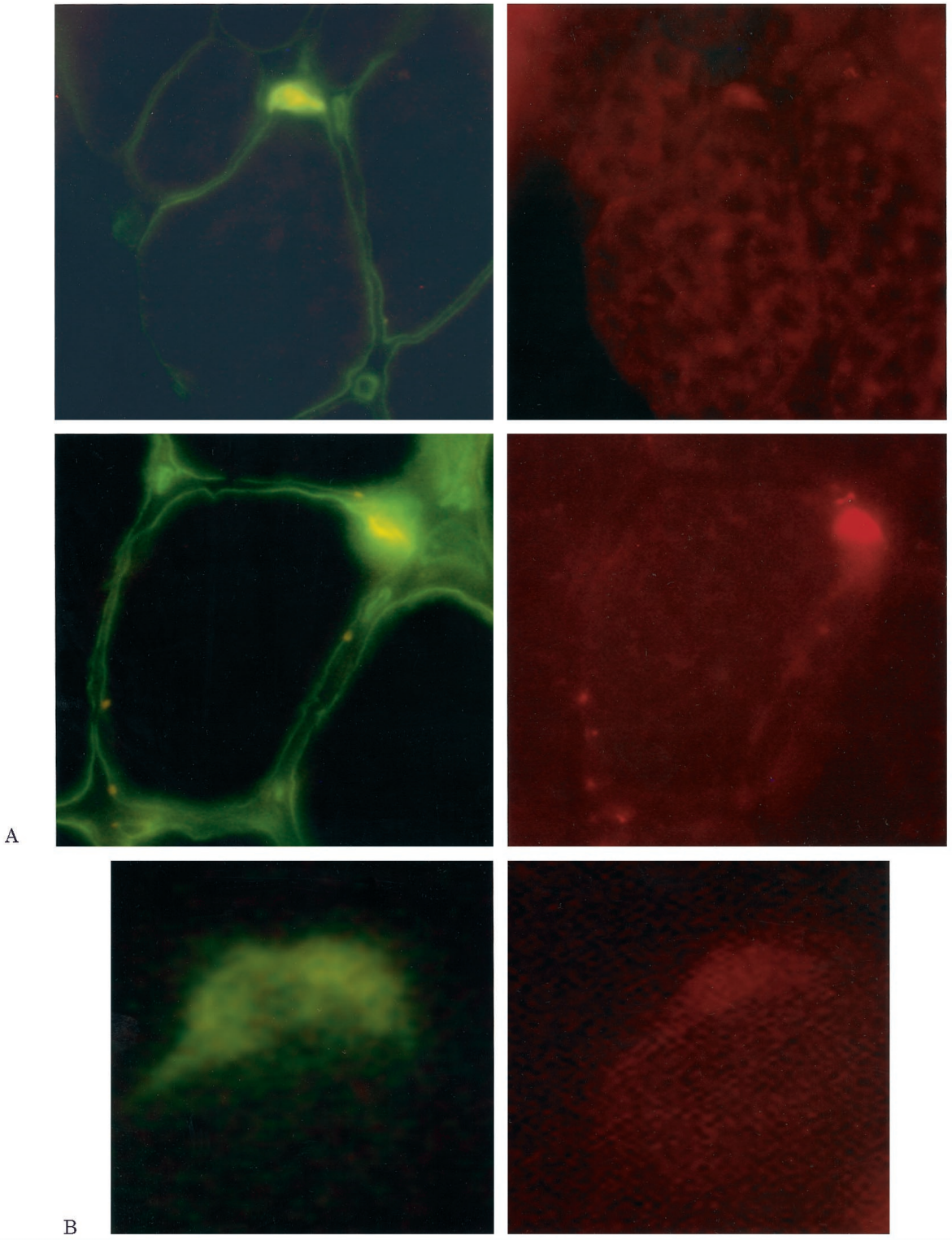

Fig 3. (A) Representative rhodamine-labeled α-bungarotoxin stains (red) for the α-subunit of the acetylcholine receptor (AChR). The α-bungarotoxin stains revealed reduced AChR density in the patient (top) compared with the end plates of control subjects (bottom). The corresponding fluorescein stains for β2 laminin (green) ascertain that the α-bungarotoxin stains were at the end plates. (B) AChR localization at the same end plate with fluorescein-labeled α-bungarotoxin (left) and an antibody directed against the γ-AChR subunit (right). Note the faint staining for the γ-AChR subunit, which was not present in controls.

decreased steadily. She lost the ability to walk between 6 and 8 years of age. At the time of examination, she showed severe generalized weakness and muscle wasting (Fig 2). She is permanently wheelchair-bound. Currently, she can perform only limited activities involving the forearm and hand muscles because of severe weakness of her upper extremities. She has nearly complete external ophthalmoplegia and mild facial weakness. Paraspinal muscle weakness resulted in progressive kyphoscoliosis. Therapy with 60 to 120 mg of pyridostigmine daily had only limited benefit. Tests for AChR antibodies were repeatedly negative. Stimulation at 3 Hz done at the age of 19 years resulted in a 22% decrement of evoked compound muscle action potentials in the deltoid muscle and a 40% decrement in the abductor digiti quinti muscle. There were no repetitive compound muscle action potentials in response to single nerve stimuli. Magnetic resonance imaging showed severe muscle wasting (see Fig 2).

At the end plates, α-bungarotoxin rhodamine-labeled staining was of reduced intensity compared with that for normal muscle (Fig 3A). Immunofluorescence studies with an antibody against the γ-AChR subunit revealed expression of the fetal subunit at the patient's end plates (see Fig 3B) but not in controls. All observed end plates of the patient were negative for the ε-AChR subunit.

Muscle histological findings revealed a marked type 2 fiber hypotrophy (Fig 4). The atrophic type 2 fibers strongly expressed vimentin but no N-CAM (CD56) (see Fig 4). Several small and large myofibers expressed neonatal myosin. Immunohistochemical analysis for proteins known to be involved in the pathogenesis of muscular dystrophies showed no abnormality. The muscle histological findings excluded the presence of muscular dystrophy in addition to the CMS in this patient.

Genetic Studies

SSCA of the whole coding region and direct sequencing revealed a homozygous insertion at nucleotide 1293 in exon 12 of the CHRNE gene (ε1293insG) in the propositus. Both parents and 3 of the patient's healthy siblings were heterozygous for the ε1293insG mutation (see Fig 1). Two siblings had no mutations, and 2 were not available for analysis.

Discussion

Engel and co-workers[2] recently described mild CMS with end-plate AChR deficiency in a 55-year-old woman. That patient had moderate ptosis and ophthalmoparesis and mild weakness of facial muscles, neck flexors, and selected limb muscles as well as abnormal fatigue on exertion. Molecular genetic analysis of AChR subunit genes revealed the presence of two different mutations in the ε-AChR subunit gene: (1) insertion of a thymine after ε-nucleotide 1101 (ε1101insT), which generates an immediate nonsense codon, and (2) insertion of a guanine after ε-nucleotide 1293 (ε1293insG), which generates three missense codons followed by a nonsense codon.

In contrast to the case reported by Engel and coworkers,[2] our patient is severely handicapped because of

Fig 4. (Left) Type 2 fiber atrophy in the patient. The small size of the type 2 fibers and the normal size of the type 1 fibers are apparent (adenosine triphosphatase reaction with preincubation at pH 4.6, magnification ×190). Representative immunoreactivity for neural cell adhesive molecules (N-CAM) (right) and vimentin (middle). The atrophic type 2 fibers strongly expressed vimentin but no N-CAM (×400). Muscle specimens were obtained from the quadriceps muscle at the age of 19 years.

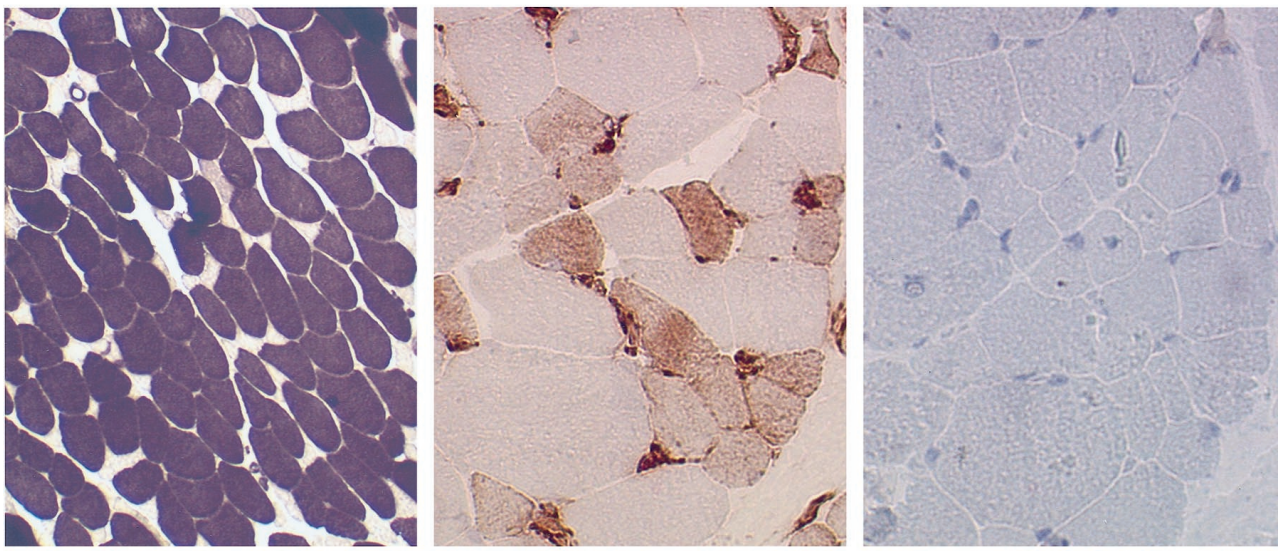

pronounced generalized weakness and muscle wasting. She was found to be homozygous for the ε1293insG-mutation. Engel and co-workers[2] performed single-channel recordings from mutant AChR ion channels harboring the ε1101insT mutation and the ε1293insG mutation, respectively.[2] Compared with the wild-type channels, ε1101insT-AChR ion channels have similar conductance and opening durations but fewer opening episodes. No channel activity was recorded from cells transfected with the ε1293insG-AChR. The phenotypic differences between the patient described by Engel and co-workers[2] and our patient are most probably a result of the different kinetic properties of these mutant AChR ion channels. In the case presented by Engel and co-workers,[2] AChR ion channels harboring the ε1101insT mutation, which leads only to mild kinetic changes, may additionally improve the neuromuscular transmission because of residual expression of the mutant ε-AChR subunit. In our patient, the homozygous ε1293insG mutation completely abolishes the function of ε-subunits translated from both CHRNE genes; thus, the neuromuscular transmission most likely depends almost completely on the expression of immature AChR ion channels, containing the γ-subunit instead of the ε-subunit. Immunofluorescence studies were indeed able to show expression of γ-subunits at the end plates of our patient. The expression of these immature γ-subunits may lead to phenotypic rescue from the potentially fatal null CHRNE mutation in our patient.[2]

The repeated muscle biopsies revealed a marked type 2 fiber atrophy (see Fig 4). Selective atrophy of type 2 fibers is a nonspecific finding that is often observed in patients suffering from neuromuscular transmission defects.[3] Remarkably, in our case, most of the atrophic type 2 fibers strongly expressed vimentin but no N-CAM (CD56). The intermediate filament vimentin is strongly expressed in fetal myotubes and can be immunohistochemically detected until week 36 of gestation.[6] Similarly, N-CAM expression occurs during myogenesis and appears in mature muscle fibers only at the neuromuscular junctions.[7] Regenerating muscle recapitulates normal phases of myofiber development, including the reappearance of strong vimentin and N-CAM immunoreactivity. This continued vimentin expression in the absence of N-CAM may indicate a disturbance in muscle fiber maturation due to impaired nerve-muscle cell interaction at the neuromuscular junction.

In conclusion, the genotype-phenotype differences in the underlying mutation haplotype may explain the variability of clinical symptoms and severity of disease observed in AChR-deficient CMS. The identification of additional patients carrying identical mutations in the heteroallelic versus homoallelic state should be helpful in further studying the complex phenotype-genotype relations in CMS patients.

This work was supported in part by grants from the Deutsche Forschungsgemeinschaft (Si472/3-1), Deutsche Gesellschaft für Muskelkranke (Freiburg i. Br.), University of Bonn (BONFOR program), and Faculty of Medicine, Johannes Gutenberg University (MAIFOR program).

We are grateful to Dr W. S. Loui for carefully reading the manuscript.

References

1. Engel AG, Ohno K, Sine SM. Congenital myasthenic syndromes: recent advances. Arch Neurol 1999;56:163–167
2. Engel AG, Ohno K, Bouzat C, et al. End-plate acetylcholine receptor deficiency due to nonsense mutations in the ε-subunit. Ann Neurol 1996;40:810–817
3. Dubowitz V. Muscle biopsy: a practical approach. 2nd ed. London: Baillière Tindall, 1985
4. Tzartos SJ, Starzinski-Powitz A. Decrease in acetylcholine-receptor content of human myotube cultures mediated by monoclonal antibodies to alpha, beta and gamma subunits. FEBS Lett 1986;196:91–95
5. Tzartos S, Langeberg L, Hochschwender S, et al. Characteristics of monoclonal antibodies to denaturated *Torpedo* and to native calf acetylcholine receptors: species, subunit and region specifity. J Neuroimmunol 1986;10:235–253
6. Sarnat HB. Vimentin and desmin in maturing skeletal muscle and developmental myopathies. Neurology 1992;42:1616–1624
7. Figarella-Branger D, Nedelec J, Pellissier JF, et al. Expression of various isoforms of neural cell adhesive molecules and their highly polysialylated counterparts in diseased human muscles. J Neurol Sci 1990;98:21–36

Acquired Hippocampal Damage after Temporal Lobe Seizures in 2 Infants

Eliane Roulet Perez, MD,* Philippe Maeder, MD,† Kathleen Meagher Villemure,‡ Virgini Chaves Vischer,* Jean-Guy Villemure, MD,§ and Thierry Deonna, MD*

Two infants developed unilateral hippocampal swelling on magnetic resonance imaging after prolonged seizures of temporal origin. Subsequent images suggested hippocampal sclerosis. The first child had febrile status epilepticus with exanthem subitum and developed refractory complex partial seizures. Histological findings after temporal lobectomy confirmed hippocampal sclerosis but also revealed sequelae of a focal encephalitis and microdysgenesis of the hippocampus. The second child had signs of brain dysgenesis, but acquired hippocampal damage affecting each side successively was documented by serial magnetic resonance imaging. These cases illustrate that different clinical conditions combining preexisting and acquired pathological characteristics can lead to hippocampal sclerosis.

Roulet Perez E, Maeder P, Meagher Villemure K, Chaves Vischer V, Villemure J-G, Deonna T. Acquired hippocampal damage after temporal lobe seizures in 2 infants. Ann Neurol 2000;48:384–387

Hippocampal sclerosis (HS) is a frequent pathological finding in adults with intractable temporal lobe epilepsy (TLE) and is being increasingly recognized in children as a result of improved magnetic resonance imaging (MRI).[1] The etiology of HS is still the subject of controversy, probably reflecting the fact that HS can be the end result of different pathological conditions,[2] including genetic predisposition[3] and acquired damage.[4]

Clinical series of surgical patients with TLE report a significantly increased incidence of prolonged or focal febrile convulsions during early childhood, suggesting that part of the process may be seizure-induced.[1,5,6]

Signs of acute unilateral hippocampal damage on MRI followed by atrophy were first reported in a child after prolonged afebrile temporal lobe seizures[7] and in a few infants after prolonged focal febrile convulsions.[8] A prospective study assessing hippocampal volumes by MRI within 48 hours after status epilepticus is ongoing, but first results indicate that hippocampal edema may develop after prolonged febrile convulsions.[9]

We report on 2 babies with unilateral swelling of the hippocampus after prolonged temporal lobe seizures and subsequent shrinkage suggesting HS. Three years later, the first child underwent temporal lobectomy for refractory TLE. Histological findings confirmed HS but also revealed hippocampal microdysgenesis and sequelae of a focal encephalitis, which was probably at the origin of the initial acute event. The second child had signs of brain dysgenesis, but acquired hippocampal damage affecting each side successively could be documented by serial MRI.

Case Reports

Case 1

This previously normal male infant presented at 6 months with a first febrile seizure lasting 40 to 50 minutes, with a left focal motor component. There was no family history of seizures. Diazepam and phenobarbital were prescribed, and excessive sedation required intubation for a few hours. After extubation, the child was reactive, with a preserved general and neurological state. During the first day, short episodes of loss of contact with left facial and arm twitching were noted. Electroencephalography (EEG) showed brief electrical seizures of right temporal origin. MRI obtained the same day was first considered normal but revealed right hippocampal swelling when reviewed (Fig 1). Lumbar puncture on admission was normal. A second LP 24 hours later showed 14 lymphocytes, without other abnormalities.

Acyclovir was given for 4 days but stopped because of lack of evidence of herpes encephalitis (negative polymerase chain reaction in cerebrospinal fluid and serum antibody titer). The child was febrile another 2 days, and on the fourth day, a cutaneous rash appeared. Exanthem subitum was diagnosed. Human herpesvirus 6 was not sought. EEG tracings on the second and sixth days showed mild right temporal slowing and normal background rhythm.

At 10 months of age, the child developed complex partial seizures. Repeat MRI at the age of 23 months showed hippocampal atrophy (see Fig 1). Despite therapy with major antiepileptic drugs, the child had 5 to 35 seizures monthly, and a right anterior temporal lobectomy was performed at 44 months.

The histological findings in the hippocampus showed focal neuronal loss and astrogliosis in the CA1 and CA3 sectors, which are usual features of HS. The fascia dentata revealed granule cell dispersion with formation of an unusual complete bilaminar organization (Fig 2). In the temporal cortex, the neuronal alignment was unremarkable, but dystrophic neurons with increased neurofilaments were seen sparsely. In addition, foci of perivascular chronic inflammatory cells, predominantly lymphocytes and plasma cells, were found in the white matter of the temporal lobe, in the hippocampus, and in the amygdala (see Fig 2). Neither viral particles nor any other infectious agent could be visualized.

From the Departments of *Pediatrics, †Radiology, ‡Pathology, and §Neurosurgery, Centre Hospitalier Universitaire Vaudois, Lausanne, Switzerland.

Received Feb 14, 2000, and in revised form Apr 19. Accepted for publication Apr 19, 2000.

Address correspondence to Dr Roulet Perez, Neuropediatric Unit, Department of Pediatrics, Office 10-928, Centre Hospitalier Universitaire Vaudois, 1011 Lausanne, Switzerland.

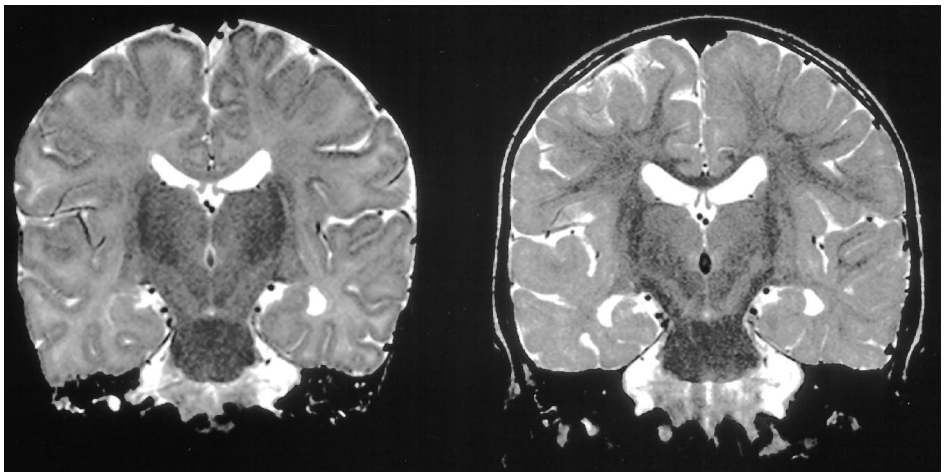

Fig 1. T2-weighted coronal MRI scans with 3-mm slice thickness. Both cuts are made through the body of hippocampi. (Left) At 6 months (response time [TR] = 5016 ms, echo time [TE] = 132 ms) and within 24 hours after febrile status epilepticus and documented seizures of the right temporal lobe, increased size of the right hippocampus with slightly increased signal and blurring of internal structures was seen. (Right) At 23 months (TR = 5400 ms, TE = 99 ms), enlarged temporal horn and slight increased signal intensity were seen, suggesting hippocampal atrophy. Note increased signal of the white matter and enlarged sulci of the right temporal lobe, correlating with gliosis found at histological examination at 44 months.

Astrogliosis was seen at every level, especially in the subpial region, and focally in the cerebral cortex and amygdala. The inflammatory changes could correspond to sequelae of the presumed viral infectious episode with which the child presented at 6 months of age.

Case 2

This male infant presented at 3 months of age with repetitive short episodes of eye blinking and apneas after a control cystoscopy and urethral valve surgery. The child had mild congenital microcephaly with delayed early milestones. A brother of the mother had mental retardation and epilepsy and cerebral palsy of unclear etiology, and he died in his 20s. On admission, the child was afebrile, and the physical examination was unremarkable. EEG showed sharp waves in the left temporo-posterior area and electrical seizures beginning at this site. Brain MRI performed within 24 hours of admission showed mildly enlarged ventricles, small subependymal nodular heterotopias, and swelling of the left hippocampus (Fig 3). Results of lumbar puncture were normal. A search for herpes encephalitis and the metabolic workup were negative. The child remained afebrile, and seizures were controlled with phenobarbital within 2 days.

At the age of 6 months, the seizures relapsed. On admis-

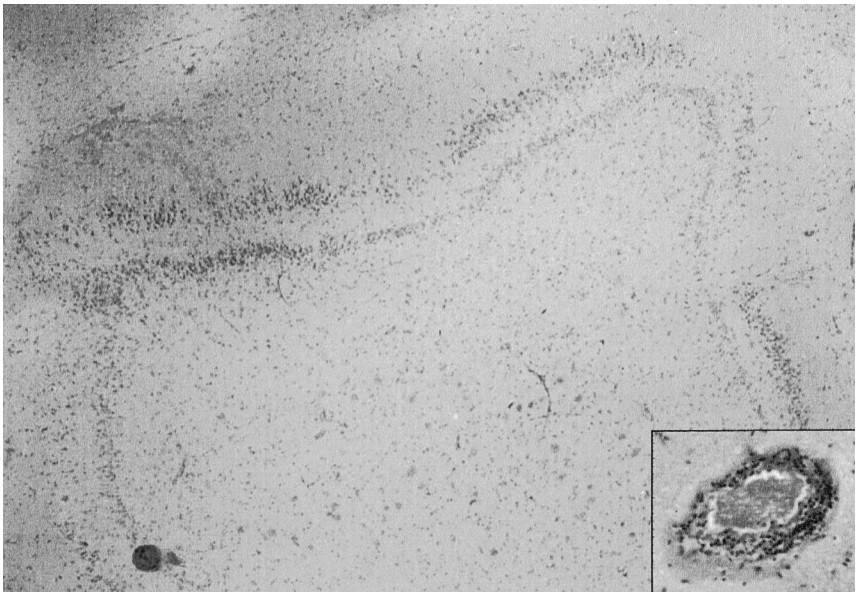

Fig 2. Hippocampal formation with bilamination of the fascia dentata (hematoxylin-eosin, ×40). (Inset) Focus of perivascular inflammatory cells (hematoxylin-eosin, ×200).

sion, the child was afebrile, and EEG again showed a temporoposterior focus but this time on the right side. Numerous electrical and electroclinical seizures with subtle changes (hypoactivity, eye deviations, chewing) of right temporoposterior onset were noted for 6 days. Isolated spikes were seen on the left side. The seizures finally stopped with antiepileptic tritherapy. A second MRI performed 10 days after admission showed acute changes in the right mesiotemporal area (see Fig 3). A further MRI at the age of 11 months showed small hippocampi on both sides, confirmed by volumetric measurements performed using published methods and normal values during development (Fig 3).[10]

Discussion

In both of these patients, we found unilateral swelling of the hippocampus on MRI performed shortly after onset of prolonged seizures originating in the corresponding temporal lobe. Follow-up MRI showed shrinkage of the affected structure, suggesting HS.

This sequence of events is important for purposes of documentation,[8] but does not answer the question of whether an underlying malformation or acquired lesion of the hippocampal region was present when the swelling occurred. In the case reported by Nohria and coworkers,[7] microdysgenesis of the temporal lobe was found, but the hippocampus was not examined.

In our first patient, histological analysis not only confirmed HS but revealed unexpected inflammatory changes in the temporal lobe and bilamination of the fascia dentata of the hippocampus (Fig 2). These signs of chronic inflammation suggest that a viral encephalitic process was at the origin of the acute event at the age of 6 months. Human herpesvirus-6, a neurotropic virus responsible for exanthem subitum, which was diagnosed clinically, is the likely agent,[11] but, unfortunately, it was not sought. The encephalitic process was mild and focal, because the baby was always alert apart from the seizures and the EEG changes were short-lived. Whether the hippocampal swelling was due to the encephalitis itself or secondary to the prolonged seizure remains open to question. If MRI performed during the acute period and later histological examination had not been available, one could have interpreted this history several years later as a typical case of TLE, with HS after prolonged febrile status epilepticus. This observation does not mean that all TLE patients with a similar history have a focal encephalitis, but this may represent a particular subgroup of young children on which prospective studies should focus.

Granule cell dispersion and bilamination have been found in patients with refractory TLE and HS who underwent surgery[12,13] but was also recently reported in 2 babies with cerebral dysgenesis and no seizures.[14] It is still unclear whether this abnormality represents an alteration of migration due to genetic factors, an unknown prenatal insult, or even an early postnatal lesion, because some granule cells are known to migrate postnatally.[12,15,16] The functional role in epilepsy of this structural abnormality situated on the afferent ex-

Fig 3. T2-weighted coronal MRI scans with 3-mm slice thickness (response time = 5400 ms, echo time = 99 ms). All cuts were made through the body of hippocampi. (Left) At 3 months and within 24 hours after onset of left temporal lobe seizures, increased size of the left hippocampus with increased signal was seen. Note the enlarged dysmorphic ventricles, including temporal horns, in a mildly microcephalic child and normal aspect of the right hippocampus. (Center) At 6 months and shortly after a prolonged period of clinical and electrical right temporal lobe seizures, increased signal in the white matter of the right fusiform gyrus was seen, with mildly thickened cortex (arrow)*, probably due to edema. There was a slight increase in the size of the right hippocampus as compared to the previous image. Note the decrease in size of the left hippocampus. (Right) At 11 months and during a seizure-free period, both hippocampi are of small size, with measured volumes of 0.7 cm^3 on the right side and 0.6 cm^3 on the left side (normal values according to age are 1.0 cm^3 and 0.9 cm^3, respectively). The size of the fusiform gyrus as compared to that in the first image is reduced, also suggesting atrophy.*

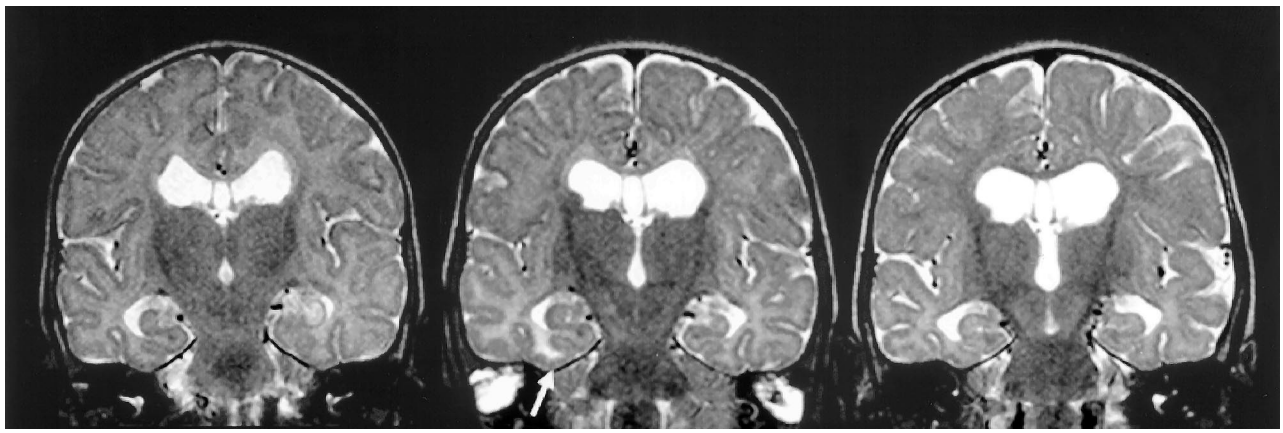

citatory pathways to the hippocampus is also unknown.[17] It may be a marker of a decreased focal epileptic threshold and contribute to maintaining an epileptic process triggered by an external agent.

The second child had definite signs of brain dysgenesis, with microcephaly, nodular heterotopias, enlarged dysmorphic ventricles, and early developmental delay. In this context, a structural abnormality of the hippocampal region preceding seizure onset can be postulated, although it was not visible on MRI. Actually, because the first MRI scan was obtained when the left side was involved, we had the opportunity of noticing the absence of a macroscopic lesion on the right side, which underwent acute changes at the age of 6 months. At this time, the gray and white matter of the fusiform gyrus adjacent to the right hippocampus seemed swollen (see Fig 3 center), presumably due to cytotoxic edema.[18]

These serial findings on MRI underline the acquired nature of at least part of the hippocampal pathological changes, which can be attributed to the prolonged clinical and subclinical focal seizure activity. An encephalitic, ischemic, or metabolic disorder can reasonably be ruled out in this case. This evolution resembles the reported clinical syndrome of early-life bilateral HS,[19] except that our child had clear preexisting pathological findings in the brain, which later evolved in two separate episodes.

Of course, these 2 cases cannot be taken as general models for explaining the pathogenesis of HS. They do illustrate the fact that different clinical conditions combining preexisting and acquired pathological characteristics[2,20] can lead to acute hippocampal damage and sclerosis, however. These complex situations can now be analyzed with early serial MRI together with EEG studies and, in some cases, histological data on the resected temporal lobe and hippocampus.

This work was supported by the Swiss National Research Fund (grant 32-5299.97 (E.R.P.)).

We thank M. Perlmutter for her assistance in the preparation of this manuscript.

References

1. Harvey AS, Grattan-Smith JD, Desmond PM, et al. Febrile seizures and hippocampal sclerosis: frequent and related findings in intractable temporal lobe epilepsy of childhood. Pediatr Neurol 1995;12:201–206
2. Mathern GW, Babb TL, Armstrong DL. Hippocampal sclerosis. In: Engel J, Jr, Pedley TA, eds. Epilepsy: a comprehensive textbook. Philadelphia: Lippicott-Raven, 1997:133–155
3. Fernandez G, Effenberger O, Vinz B, et al. Hippocampal malformation as a cause of familial febrile convulsions and subsequent hippocampal sclerosis. Neurology 1998;50:909–917
4. Jackson GD, McIntosh AM, Briellmann RS, et al. Hippocampal sclerosis studied in identical twins. Neurology 1998;51: 78–84
5. French JA, Williamson PD, Thadani M, et al. Characteristics of medial temporal lobe epilepsy. I. Results of history and physical examination. Ann Neurol 1993;34:774–780
6. Shinnar S. Prolonged febrile seizures and mesial temporal sclerosis. Ann Neurol 1998;43:411–412
7. Nohria V, Lee N, Tien RD, et al. Magnetic resonance imaging evidence of hippocampal sclerosis in progression: a case report. Epilepsia 1994;35:1332–1336
8. VanLandingham KE, Heinz ER, Cavazos JE, et al. Magnetic resonance imaging evidence of hippocampal injury after prolonged focal febrile convulsions. Ann Neurol 1998;43:413–426
9. Scott RC, Gadian G, Neville B, et al. Hippocampal volume within 48 hours of status epilepticus. Eur J Pediatr Neurol 1999;3:A17 (Abstract)
10. Utsunomiya H, Takano K, Okazaki M, et al. Development of the temporal lobe in infants and children: analysis by MR-based volumetry. AJNR Am J Neuroradiol 1999;20:717–723
11. Suga S, Yoshikawa T, Asano Y, et al. Clinical and virological analyses of 21 infants with exanthem subitum (roseola infantum) and central nervous system complications. Ann Neurol 1993;33:597–603
12. Houser CR. Granule cell dispersion in the dentate gyrus of humans with temporal lobe epilepsy. Brain Res 1990;553:195–204
13. Raymond AA, Fish DR, Stevens JM, et al. Association of hippocampal sclerosis with cortical dysgenesis in patients with epilepsy. Neurology 1994;44:1841–1845
14. Harding BJ, Thom M. Bilateral granule cell dispersion in the hippocampi of 3 infants at autopsy. J Neuropathol Exp Neurol 1999;58:519 (Abstract)
15. Mathern GW, Leite JP, Pretorius JK, et al. Children with severe epilepsy: evidence of hippocampal neuron losses and aberrant mossy fiber sprouting during postnatal granule cell migration and differentiation. Dev Brain Res 1994;78:70–80
16. Babb TL. Hippocampal sclerosis and dual pathology: experimental and clinical evidence for developmental lesions. In: Tuxhorn I, Holthausen H, Boenigk H, eds. Pediatric epilepsy syndromes and their surgical management. London: John Libbey, 1997:227–233
17. Meagher-Villemure K, Villemure JG. Hippocampal abnormalities preceding hippocampal sclerosis in epileptic patients. Can J Neurol Sci 1999;26:344 (Abstract)
18. Henry TR, Drury I, Brunberg JA, et al. Focal cerebral magnetic resonance changes associated with partial status epilepticus. Epilepsia 1994;35:35–41
19. DeLong GR, Heinz ER. The clinical syndrome of early life bilateral hippocampal sclerosis. Ann Neurol 1997;42:11–17
20. Lewis DV. Febrile convulsions and mesial temporal sclerosis. Curr Opin Neurol 1999;12:197–201

Gene Polymorphism Affecting α1-Antichymotrypsin and Interleukin-1 Plasma Levels Increases Alzheimer's Disease Risk

Federico Licastro, MD,* Steve Pedrini, MSc,* Cinzia Ferri, MSc,† Valeria Casadei, MD,† Marzia Govoni, MSc,* Annalisa Pession, MSc,* Francesca Luisa Sciacca, MD,† Fabrizio Veglia, PhD,† Giorgio Annoni, MD,‡ Massimiliano Bonafè, MD,* Fabiola Olivieri, MSc,§ Claudio Franceschi, MD,§ and Luigi Maria Edoardo Grimaldi, MD†

Plasma levels of α1-antichymotrypsin (ACT) and interleukin-1β (IL-1β) were increased in patients with probable Alzheimer's disease (AD). A common polymorphism within ACT and IL-1β genes affected plasma levels of ACT or IL-1β, and AD patients with the ACT T,T or IL-1β T,T genotype showed the highest levels of plasma ACT or IL-1β, respectively. The concomitant presence of the ACT T,T and IL-1β T,T genotypes increased the risk of AD (odds ratio: 5.606, confidence interval: 1.654–18.996) and decreased the age at onset of the disease.

Licastro F, Pedrini S, Ferri C, Casadei V, Govoni M, Pession A, Sciacca FL, Veglia F, Annon G, Bonafè M, Olivieri F, Franceschi C, Grimaldi LME. Gene polymorphism affecting α1-antichymotrypsin and interleukin-1 plasma levels increases Alzheimer's disease risk. Ann Neurol 2000;48:388–391

The major cause of cognitive deterioration in the elderly is Alzheimer's disease (AD), a disease with complex and heterogeneous pathogenetic mechanisms.[1] Genetic factors have been found associated with the sporadic or nonfamilial form of the disease,[2] and allele 4 of apolipoprotein E (ApoE)[3,4] significantly increases the risk of AD. Other genetic and environmental factors might also be implicated in the disease, because allelic variants of a few molecules could not account for all sporadic AD.

Molecules that regulate inflammation are of great interest, because inflammation is often associated with neurodegenerative hallmarks in the AD brain. Reactive astrocytosis is present in the cortex and hippocampus of AD brain,[5] and activated glia are localized within or near AD lesions.[6] Cytokines released by astroglia may play a role in neuronal death,[7] and interleukin-1 (IL-1)–containing microglia are increased in Down's syndrome and AD brains.[8] Activated astrocytes surrounding amyloid plaques express increased α1-antichymotrypsin (ACT) messenger RNA,[9] an acute phase protein, and increased ACT protein levels are present in AD brains.[10] Moreover, ACT and IL-1 may be functionally linked, because IL-1 promoted overexpression of ACT messenger RNA in activated astrocytes.[11] Subjects taking anti-inflammatory medications have a reduced risk of developing AD.[12]

Markers of abnormal immune regulation such as increased blood levels of IL-1β[13] and ACT[14] in patients with AD have also been found, and the polymorphic alleles in the promoter region of IL-1α and IL-1β genes have been shown to increase AD risk.[15] Therefore, inflammation might be intrinsically associated with neurodegenerative processes leading to AD, and ACT and IL-1β molecules might have a special role in AD pathogenesis.

To further investigate the relevance of these molecules in sporadic AD, the effects of ACT and IL-1β gene polymorphisms on plasma levels of ACT and IL-1β and on the risk of developing AD were investigated.

Patients and Methods

Patients and Controls

Diagnosis of probable AD was performed according to standard clinical procedures and followed the NINCDS-ADRDA[16] and Diagnostic and Statistical Manual of Mental Disorders (third revised edition) criteria.[17] Cognitive performances and alterations were measured according to the Mini-Mental State Evaluation (MMSE) and Global Deterioration Scale. Only controls and AD patients without clinical signs of systemic inflammation (eg, normal body temperature or absence of concomitant inflammatory disease) were chosen. AD patients or controls with an abnormal erythrocyte sedimentation rate or blood albumin, transferrin, or C-reactive protein levels were not included. According to this procedure, 118 patients with probable AD (mean [±SE] age, 74 ± 1 years, MMSE score, 14 ± 0.8) and 144 controls (mean age, 83 ± 1 years, MMSE score, >26) entered the pilot study on plasma ACT and IL-1β. The ACT and IL-1β genotype investigation included 281 patients with probable AD (172 women, mean age, 76 ± 1 years; 109 men, mean age, 72 ± 1 years; MMSE score: 15 ± 0.5) and 201 nondemented controls (64 women, mean age, 75 ± 1 years; 137 men, mean age, 66 ± 1 years; age range, 50–92 years; MMSE score, >26). Patients and controls were Caucasian and recruited from north-

From the *Dipartimento di Patologia Sperimentale, School of Medicine, University of Bologna, and †Neuroimmunology Unit, Department of Neuroscience, San Raffaele Hospital and ‡Department of Geriatrics, University of Milan, Milan, and §Instituto Nationale Ricerca e Ricovero Anziani, Ancona, Italy.

Received Feb 9, 2000, and in revised form Apr 6 and Apr 24. Accepted for publication Apr 24, 2000.

Address correspondence to Dr Licastro, Dipartimento di Patologia Sperimentale, School of Medicine, University of Bologna, Via San Giacomo 14, 40126 Bologna, Italy.

ern Italy. Informed consent from each control and a relative of each AD patient was obtained.

Plasma Levels of ACT and IL-1β

Blood levels of IL-1β (Endogen, Milan, Italy) and ACT (The Binding Site, Birmingham, UK) were measured as previously described.[18]

Genetic Screening

DNA was obtained from blood mononuclear cells by a commercial kit (QiAmp blood kit; Kagan, Crawley, UK). The triallelic Apoe ε2–4 polymorphism was assessed by a polymerase chain reaction–based method.[19] The ACT biallelic polymorphism in the signal peptide (15 Ala → Thr) and the C-to-T restriction fragment length polymorphism within the IL-1β promoter region were assessed as previously described.[15,19]

Statistical Analysis

Genotype and allele distribution were analyzed by χ^2 test. The odds ratio (OR) was also calculated as described elsewhere.[19] The Hardy-Weinberg equilibrium was verified in both AD and control populations. ACT and IL-1β plasma levels were compared by ANOVA One Way. The adjusted OR was estimated by logistic regression analysis (Cochran-Manel-Haenszel statistics). The effect of genotypes on the age at onset of AD was assessed by the Kaplan-Meier analysis and log rank statistic.

Results

Plasma proteins were reduced in demented patients (AD, 41 ± 1 g/L; controls, 50 ± 1 g/L; $p < 0.0001$). Therefore, plasma ACT was calculated as the percentage of plasma protein to minimize variability and was increased in patients (AD, 1.005 ± 0.03%; controls, 0.778 ± 0.04%; $p < 0.001$). As shown in Figure A, among AD patients, those with the ACT T,T genotype had the highest levels of the serpin (T,T vs A,A genotype; $p < 0.05$). Levels of ACT from AD patients with the ACT T,T genotype were still increased when data were expressed as absolute values (ACT T,T: 444 ± 20 mg/L vs ACT A,A + A,T: 382 ± 18 mg/L; $p = 0.05$), although no difference in total plasma protein between AD groups (42 ± 2, 41 ± 2, and 41 ± 2 g/L, respectively) was present.

Plasma IL-1β was increased in patients (AD, 0.479 ± 0.15 pg/ml, controls, 0.14 ± 0.02 pg/ml; $p < 0.02$), was detectable in a larger proportion of AD patients than controls (14% vs 0.7%, respectively; $p = 0.0001$) and was highest in AD patients with the IL-1β T,T genotype (T,T vs C,C genotype; $p < 0.03$; see Fig B). Differences between the 3 AD groups were also present when IL-1β was expressed as a percentage of plasma protein (C,C = 7%, C,T = 12%; T,T = 36% × 10^{-10}).

We then investigated whether any combination of the ACT A,T and IL-1β C,T genotypes might modify the risk of AD. The concomitant presence of both

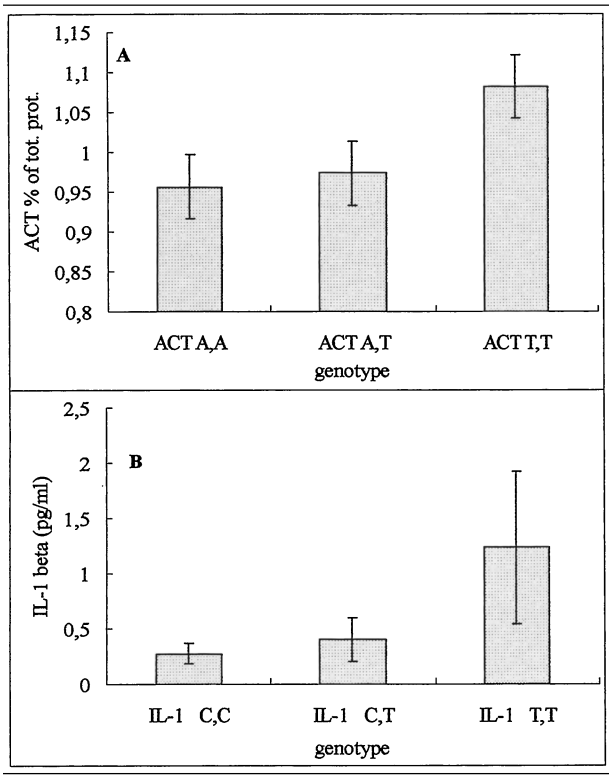

Fig. (A) Effect of α1-antichymotrypsin (ACT) A,T genotypes on plasma levels of ACT (expressed as percentage of total plasma protein) in Alzheimer's disease (AD) patients (AD with ACT T,T vs AD with ACT A,A + A,T; $p < 0.05$*). (B) Effect of interleukin-1β (IL-1β) C,T genotypes on plasma levels of IL-1β in AD (AD with IL-1β T,T vs AD with IL-1β C,C + C,T;* $p < 0.03$*).*

ACT T,T and IL-1β T,T genotypes significantly increased the risk of AD (Table; OR, 5.606, CI, 1.654–18.996, $p = 0.002$) independently from the ApoE4 status (ApoE4–adjusted OR, 10.009, CI, 2.779–36.437; $p = 0.001$). The presence of the ACT T,T genotype alone or the IL-1β T,T genotype alone conferred a slight increase in the risk for the disease (OR, 2.56, CI, 1.3–5.2, $p = 0.009$ and OR, 2.33, CI, 1.3–4.18, $p = 0.004$, respectively).

The presence of both genotypes slightly decreased the age at onset of AD in patients older than 65 years (mean age of ACT T,T/IL-1βT,T carriers, 68.86 ± 2.25 years; mean age of noncarriers, 73.28 ± 0.69 years; $p = 0.062$). This difference was at the limit of statistical significance, because the number of ACT T,T/IL-1βT,T homozygous patients was small. When the analysis was restricted to late onset AD (age > 65 years) with the ACT T,T genotype, a small but statistically significant decrease in age at onset of the disease was also observed (ACT T,T: 70.37 ± 1.25 years, ACT A carriers: 73.72 ± 0.77 years; $p = 0.0241$).

Table. Frequency of the α1-Antichymotrypsin T,T/Interleukin-1β T,T Genotypes in Alzheimer's Disease Patients and Nondemented Controls

	Subjects with α1-Antichymotrypsin T,T/Interleukin-1β T,T Genotypes	n	Odds Ratio	*p* (95% CI)
Alzheimer's disease patients	22 (7.8%)[a]	281	5.606	0.0001 (1.654–18.996)
Controls	3 (1.5%)[a]	201		

[a]Statistical significance according to χ^2 test: $p = 0.002$.

Apolipoprotein E4–adjusted odds ratio in subjects with the α1-antichymotrypsin T,T/interleukin-1β T,T genotypes: 10.009, confidence interval: 2.779–36.437; $p = 0.001$.

Conclusions

Our findings suggest that different genetic backgrounds might affect diverse abilities of synthesizing, releasing, or absorbing inflammation-related factors in patients with AD. Polymorphisms of ACT and IL-1β genes influenced the blood turnover of these molecules in AD, because they were associated with different levels of circulating ACT or IL-1β. At the moment, we cannot ascribe the increment of blood ACT or IL-1β levels to an obvious activation of peripheral immunocytes. A previous investigation[18] showed no association between metabolic activation of the reticular endothelial cell system and increased levels of ACT and IL-1β in AD and suggested a possible brain origin of these factors. Furthermore, patients were selected to minimize the presence of subclinical peripheral inflammation.

In the Italian population, the ACT T,T and IL-1β T,T genotypes were slightly and independently increased in patients with AD as shown here and elsewhere.[15,19] The concomitant presence of these genotypes was increased in AD patients and identified a group of subjects with an elevated risk of late-onset AD. The present data support the notion that ACT and IL-1β genes might be functionally linked to pathogenetic mechanisms associated with AD. The diverse genetic backgrounds of these molecules might influence the risk of developing AD by differentially affecting the brain capacity to respond to inflammatory stimulation.

Our recent observations showing that ACT plasma levels in AD patients positively correlated with the degree of cognitive deterioration[18] as assessed by the MMSE or Global Deterioration Scale and that brain ACT correlated with the number of activated astrocytes[20] indirectly support these speculations. It is unclear whether ACT increase is a primary or a secondary event in AD; nevertheless, it seems to be associated with cognitive deterioration, because ACT levels were also elevated in nondemented elderly subjects with marginal cognitive impairment (data not shown).

The group of patients with both ACT T,T and IL-1β T,T genotypes was small but showed a high risk of AD and a decreased age at onset of the disease. This age-related effect was only observable in patients older than 65 years. Therefore, genetic background, brain inflammation, and age might differentially interact in subgroups of patients, and inflammation might play a special role in sporadic late-onset AD.

Finally, we speculated that patients with diverse genetic backgrounds for inflammatory molecules might differentially benefit from anti-inflammatory therapies aimed at delaying the progress of the disease.

This research was supported by the Italian MURST (40% and 60%) and Italian ARAD.

References

1. Katzman RN. Medical progress: Alzheimer's disease. N Engl J Med 1986;274:964–973
2. Rubinsztein DC. The genetics of Alzheimer's disease. Prog Neurobiol 1997;52:447–454
3. Corder EH, Saunders AM, Strittmatter WJ, et al. Gene dose of apolipoprotein E type 4 allele and the risk of Alzheimer's disease in late onset families. Science 1993;261:921–923
4. Poirier J, Davignon J, Bouthillier D, et al. Apolipoprotein E polymorphism and Alzheimer's disease. Lancet 1993;342:697–699
5. Beach TG, Walker R, McGeer EG. Patterns of gliosis in Alzheimer's disease and aging cerebrum. Glia 1989;2:420–436
6. McGeer PL, Rogers J, McGeer EG. Neuroimmune mechanisms in Alzheimer's disease pathogenesis. Alzheimer Dis Assoc Disord 1994;8:149–158
7. Griffin WS, Sheng JG, Royston MC, et al. Glial-neuronal interactions in Alzheimer's disease: the potential role of a "cytokine cycle" in disease progression. Brain Pathol 1998;818: 65–72
8. Griffin WS, Stanley LC, Ling C, et al. Brain interleukin-1 and S-100 immunoreactivity are elevated in Down's syndrome and Alzheimer's disease. Proc Natl Acad Sci USA 1989;86:7611–7615
9. Abraham CR, Selkoe DJ, Potter H. Immunochemical identification of the serine protease inhibitor alpha-1-antichymotrypsin in the brain amyloid deposits. Cell 1988;52:487–502
10. Licastro F, Campbell IL, Kincaid C, et al. A role for apoE in regulating the levels of alpha-1-antichymotrypsin in the aging mouse brain and in Alzheimer disease. Am J Pathol 1999;155: 869–875
11. Lieb K, Fielbich BL, Schaller H, et al. Interleukin-1β and tumor necrosis factor-α induce expression of α_1-antichymotrypsin in human astrocytoma cells by activation of nuclear factor-kappa B. J Neurochem 1996;67:2039–2044
12. Breitner JCS, Gau BA, Welsh KA, et al. Inverse association of

anti-inflammatory treatments and Alzheimer's disease. Neurology 1994;44:227–232
13. Alvarez XA, Franco A, Fernandez-Novoa F, Cacabelos R. Blood levels of histamine, IL-1β and TNF-α in patients with mild to moderate Alzheimer disease. Mol Chem Neuropathol 1996;29: 237–252
14. Licastro F, Morini MC, Polazzi E, Davis LJ. Increased serum α-1-antichymotrypsin in patients with probable Alzheimer's disease: an acute phase reactant without the peripheral acute phase response. J Neuroimmunol 1995;57:71–75
15. Grimaldi LME, Casadei VM, Ferri C, et al. Association of early onset Alzheimer's disease with an interleukin-1α gene polymorphism. Ann Neurol 2000;47:351–365
16. McKhann G, Drachman D, Folstein M, et al. Clinical diagnosis of Alzheimer's disease: report of the NINCDS-ADRDA Work Group under the auspices of Department of Health and Human Services Task Force on Alzheimer's Disease. Neurology 1984;34:939–944
17. American Psychiatric Association. Diagnostic and Statistical Manual of Mental Disorders: DSM-III-R, 3rd revised ed. Washington, DC: American Psychiatric Association, 1987
18. Licastro F, Pedrini S, Caputo L, et al. Increased plasma levels of interleukin-1, interleukin-6 and α-1-antichymotrypsin in patients with Alzheimer's disease: peripheral inflammation or signals from the brain? J Neuroimmunol 2000;103:97–102
19. Licastro F, Pedrini S, Govoni M, et al. Apolipoprotein E and α-1-antichymotrypsin allele polymorphism in sporadic and familial Alzheimer's disease. Neurosci Letters 1999;270:129–132
20. Licastro F, Mallory M, Hansen LA, Masliah E. Increased levels of alpha-1-antichymotrypsin in brains of patients with Alzheimer's disease correlate with activated astrocytes and are affected by APOE 4 genotype. J Neuroimmunol 1998;88:105–110

Limited Donepezil Inhibition of Acetylcholinesterase Measured with Positron Emission Tomography in Living Alzheimer Cerebral Cortex

David E. Kuhl, MD,* Satoshi Minoshima, MD, PhD,* Kirk A. Frey, MD, PhD,*† Norman L. Foster, MD,† Michael R. Kilbourn, PhD,* and Robert A. Koeppe, PhD*

Based on surrogate assays of peripheral red blood cells, reports state that widely prescribed doses of donepezil hydrochloride provide nearly complete inhibition of cerebral cortical acetylcholinesterase activity in the treatment of Alzheimer's disease (AD). To test this, direct positron emission tomography measures of cerebral acetylcholinesterase activity were made in AD patients before and after treatment with donepezil (5 and 10 mg/day) for at least 5 weeks and compared with similar measures in normal controls who were untreated or after acute administration of another AChE inhibitor, physostigmine salicylate (1.5 mg/hr). After physostigmine, acetylcholinesterase inhibition averaged 52% in normal cerebral cortex. After donepezil, cerebral cortical inhibition in AD brain averaged only 27%. Clinical trials of this donepezil dose schedule are not testing the effect of nearly complete cerebral cortical inhibition.

Kuhl DE, Minoshima S, Frey KA, Foster NL, Kilbourn MR, Koeppe RA. Limited donepezil inhibition of acetylcholinesterase measured with positron emission tomography in living Alzheimer cerebral cortex. Ann Neurol 2000;48:391–395

The use of cholinomimetic drugs to improve cognitive functioning in Alzheimer's disease (AD) is based on presynaptic cholinergic deficits found consistently in AD cerebral cortex as well as studies of acetylcholine (ACh) in animal and human behavior.[1] A common rationale is to increase the availability of ACh within

From the *Division of Nuclear Medicine, Department of Internal Medicine, and †Department of Neurology, University of Michigan, Ann Arbor, MI.

Received Mar 1, 2000, and in revised form Apr 19. Accepted for publication May 11, 2000.

Address correspondence to Dr Kuhl, Division of Nuclear Medicine, University of Michigan Hospital, Room B1 G505/0028, Ann Arbor, MI 48109-0028.

cholinergic synapses of cerebral cortex and hippocampus through inhibition of its hydrolysis by acetylcholinesterase (AChE). Lacking direct measures, the relation between drug dose and extent of the central AChE inhibition process has been inferred from peripheral measures, such as red blood cell (RBC) membrane AChE assays, which serve as convenient but uncertain surrogate markers of central inhibition. Instead, direct measures might forestall unwarranted assumptions of drug efficiency and identify potential for improvement. These are timely considerations. It is anticipated that the widespread use of new second-generation inhibitor drugs, at efficacious doses, will establish whether cholinomimetic therapy can palliate and even perhaps alter disease progression in AD.

Donepezil hydrochloride (Aricept TM, Eisai Inc, Teaneck, NJ), a specific inhibitor of AChE, is a widely prescribed treatment of mild to moderate AD because it has been shown to be more effective than placebo in large double-blind clinical trials, lacks serious adverse effects, and is convenient to use.[2] Finding an 80 to 90% plateau of RBC enzyme inhibition at higher plasma concentrations, investigators concluded that in many patients a donepezil dose of no more than 5 or 10 mg/day already imparted nearly complete central inhibition.[2] To test this, direct positron emission tomography (PET) measures[3] of cerebral AChE activity were made in AD patients before and after treatment with donepezil (5 and 10 mg/day) and compared with similar measures in normal controls who were untreated or who had received another AChE inhibitor, physostigmine salicylate (1.5 mg/hr).

Patients and Methods

The patients (n = 9) had a clinical diagnosis of probable AD[4] made by a neurologist and were taking no medications with actions known to affect the central cholinergic system. The characteristics of those whose donepezil dosage was escalated from 5 to 10 mg/day (n = 6; mean age, 68 ± 9 years; mean age at onset, 63 ± 10 years; Clinical Dementia Rating[5] [CDR], 1.7 ± 0.5; Mini-Mental State Examination[6] [MMSE] score, 18 ± 4) were similar to those of the overall group (n = 9; mean age, 69 ± 7 years; mean age at onset 65 ± 9 years; CDR, 1.4 ± 0.5; MMSE score, 18 ± 4). The elderly normal control group (n = 14; mean age 66 ± 7 years) had no history of significant general medical, neurological, or psychiatric illness; head injury with loss of consciousness; or drug or alcohol dependence. They were taking no medications with central nervous system actions. The study was approved by the Institutional Review Board. Written informed consent was obtained from all subjects, their spouses, or their legal guardians.

Data were acquired from patients and controls using a PET scanner (Siemens ECAT EXACT-47, CTI Inc, Knoxville, TN) with interplane septa retracted (three-dimensional [3D] mode). Details of preparation of *N*-[^{11}C]methylpiperidin-4-yl propionate ([^{11}C]PMP),[7] data acquisition, and analysis were as reported previously,[3] with the exception that all patients and controls were scanned in the 3D mode rather than the 2D mode. A three-compartment model was used to yield pixel-by-pixel estimates of k_3 (AChE hydrolysis rate). Regional values of k_3 were extracted using the 3D stereotactic surface projection (3D-SSP) technique[8] and stereotactically predefined volumes of interest (VOIs). Cerebral cortical k_3 data from AD patients were calculated, expressed as percentage of mean normal, and compared with control values using one-tailed *t* statistics. Posttreatment k_3 data were also calculated for four anatomical zones (cerebral cortical, striatal, thalamic, and pontocerebellar), expressed as percentage decrease from pretreatment values (inhibition), and compared with pretreatment values using one-tailed paired *t* tests corrected for multiple comparisons.

The first [^{11}C]PMP scan was performed on each of 9 AD patients before starting donepezil treatment (5 mg/day). A second scan was performed 5 to 10 weeks (mean, 7 weeks) later. In 6 of these patients, a third scan was performed 8 to 26 weeks (mean, 13 weeks) after donepezil dosage had been increased from 5 to 10 mg/day. To determine reproducibility of the method, an additional 6 normal control subjects had repeat [^{11}C]PMP scans after an interval of 4 to 12 weeks (mean, 8 weeks).

Results

Figure 1 shows the distribution of AChE reduction (*Z*-scored) in whole brain of those AD patients (n = 6) who had three scans—before treatment and at two different levels of donepezil dosage. Even before treatment, AChE activity was widely reduced in cerebral cortex, most prominently in temporal cortex, but was not reduced in striatum, thalamus, or pontocerebellar structures. AChE activity was reduced further after donepezil treatment at 5 mg/day, uniformly across cerebral cortex and even more pronounced in striatum, thalamus, and pontocerebellar structures. With donepezil dose escalation to 10 mg/day, there was no significant incremental effect on cerebral cortical AChE activity.

In Figure 2, AChE activity in cerebral cortex is expressed as a percentage of the normal mean value. In normal cerebral cortex, the coefficient of variation was 19% for intersubject (n = 14) measurements of AChE activity, but duplicate intrasubject measures (n = 6) at 2-month intervals differed by only 6 ± 3% (mean ± SD of the absolute value of the percentage difference between the two scans). In AD cerebral cortex (Fig 2), AChE activity was already reduced to 80 ± 14% mean normal ($p = 0.003$) before treatment (n = 9), was reduced further to 59 ± 9% mean normal after 5 mg/day donepezil (n = 9), but remained at 56 ± 9% mean normal after escalation of the donepezil dose to 10 mg/day (n = 6).

The Table lists calculated AChE inhibition (percentage decrease from pretreatment values) based on these [^{11}C]PMP PET measures for four anatomical zones in AD patients (n = 6) who had donepezil dose escala-

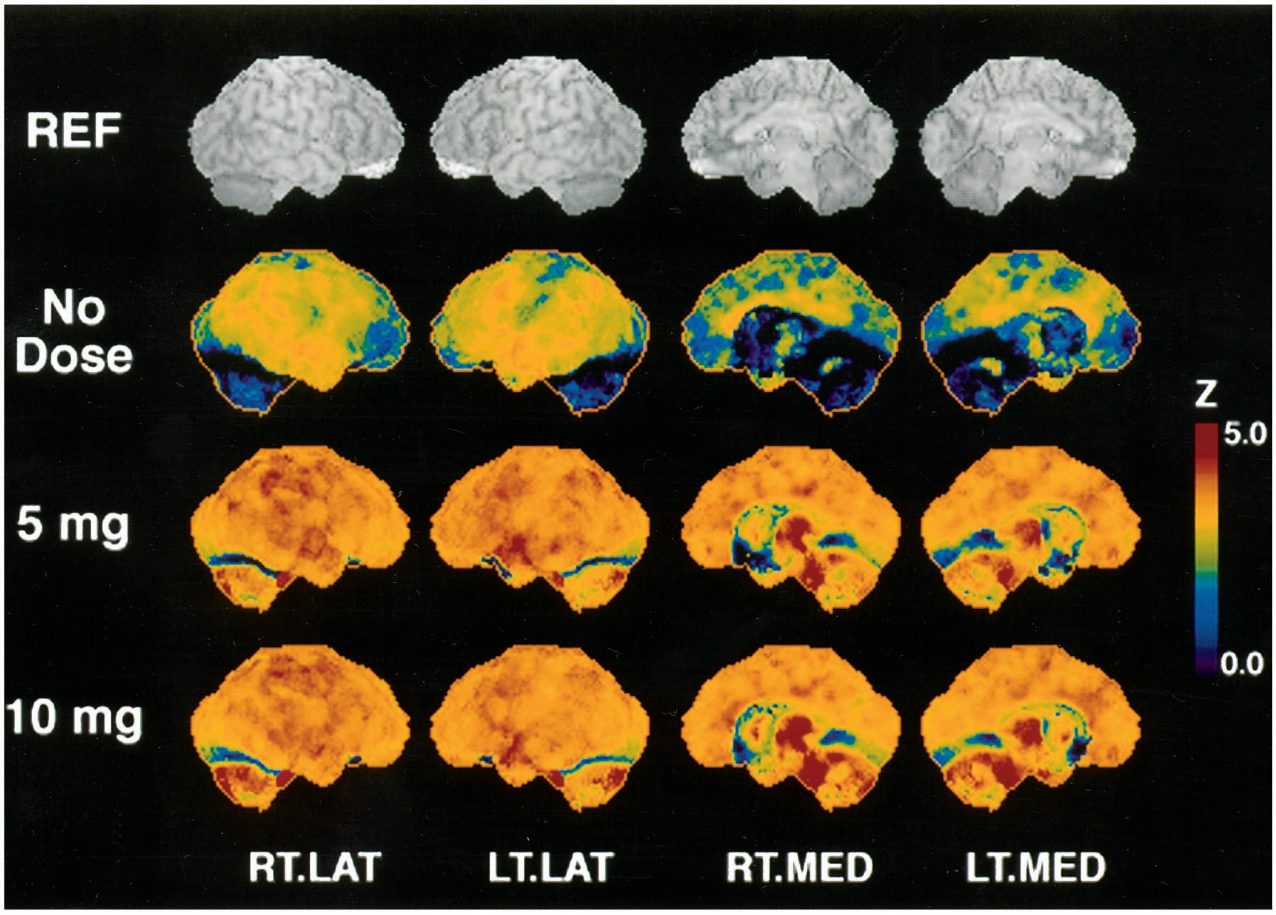

Fig 1. Cerebral acetylcholinesterase (AChE) activity before and after donepezil treatment in Alzheimer disease subjects (n = 6) compared with untreated normal controls (n = 14). N-*[*^{11}*C]methylpiperidin-4-yl propionate ([*^{11}*C]PMP)* k_3 *summations are shown as* Z *scores (converted from paired* t *statistics) of the differences from normal, plotted as three-dimensional stereotactic surface projections. In cerebral cortex, AChE activity was reduced widely even before treatment, then reduced further and more uniformly after the 5-mg/day donepezil dose schedule, but it remained unchanged after donepezil dose escalation to 10 mg/day. In striatal, thalamic, and pontocerebellar structures, reductions in AChE activity were absent before treatment but exceeded cerebral cortical reductions after donepezil.*

Table. Inhibition of Cerebral Acetylcholinesterase Activity Measured Using N-*[*^{11}*C]methylpiperidin-4-yl Propionate, Positron Emission Tomography*

	Donepezil in Alzheimer's Disease (n = 6)		Physostigmine in Controls[3] (n = 5)
Zones	5 mg/day	10 mg/day	1.5-mg Infusion
Cerebral cortical	26 ± 12[b]	27 ± 11[b]	52 ± 9[c]
Striatal	36 ± 18[b]	47 ± 9[b]	44 ± 18[b]
Thalamic	44 ± 5[c]	50 ± 4[c]	61 ± 9[c]
Pontocerebellar	51 ± 7[c]	61 ± 6[d]	64 ± 6[d]

[a]Posttreatment k_3 expressed as percentage decrease (mean ± SD) from pretreatment value.
[b]$p < 0.01$, [c]$p < 0.001$, [d]$p < 0.0001$, by single-tailed paired *t* tests corrected for multiple comparisons.

tion and in normal controls (n = 5) who had physotigmine infusions. After an acute physostigmine infusion (1.5 mg/hr), AChE inhibition in normal cerebral cortex measured 52 ± 9% (mean ± SD). After donepezil doses of 5 or 10 mg/day for at least 5 weeks, mean AChE inhibition in AD cerebral cortex measured only 26 ± 12% and 27 ± 11%, respectively.

Discussion

In individual normal subjects, PET measures of cerebral cortical AChE activity repeated after 2-month intervals differed by only 6%. This level of precision is suitable for test–retest determination of inhibitor effects. The large variance found among normal subjects (19%) matched the biological variation (17%) of cholinergic neurons counted in postmortem nucleus basalis using immunocytochemistry.[9] In PET measures of AD

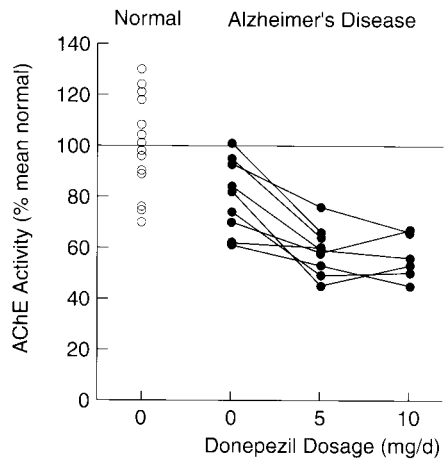

Fig 2. Cerebral cortical acetylcholinesterase (AChE) activity measured in untreated normal controls (n = 14) and in Alzheimer's disease subjects before and after 5-mg/day (n = 9) and 10-mg/day (n = 6) donepezil treatment schedules. These PET measures of AChE activity are the regional values of N-*[^{11}C]methylpiperidin-4-yl propionate ([^{11}C]PMP) k3 expressed as a percentage of the mean normal value. AChE activity was already reduced before treatment, was reduced more after 5 mg/day of donepezil, but declined no further after escalation of the donepezil dose to 10 mg/day.*

brain before treatment, cholinergic deficits varied regionally. Cerebral cortex was involved, but other parts were not. These results agree with previous reports[3,10,11] that the cholinergic deficit in AD is confined to a diffuse distribution within cerebral cortex, where it is most severe in the temporal cortex.

Inhibition of AChE after physostigmine treatment was nearly uniform throughout gray matter structures of normal brain. This was not so in AD brain after donepezil treatment. Inhibition was considerably less in cerebral cortex than in striatum, thalamus, and pontocerebellum, structures that are relatively spared in AD (see Table). Donepezil dose schedules of 5 and 10 mg/day produced less AChE inhibition in AD cerebral cortex (only 26% and 27%, respectfully) than has been inferred from surrogate RBC AChE assays (64% and 77%, respectively) as applied in extensive clinical trials.[2]

The low donepezil response found in AD cerebral cortex cannot be explained as an artifact of the method. Similar results from 9 patients make dose noncompliance an unlikely factor. Likewise, the findings cannot be attributed to systematic underestimation inherent in PET mapping. The same PET method has demonstrated better than 50% reductions in cerebral cortical AChE in normal controls treated with physostimine and in some untreated AD patients.[3] Atrophy has little effect on this AChE measure.[3] [^{11}C]PMP is a very selective substrate for AChE,[12] and even large increases in cortical butyrlcholinesterase activity[13] could not account for the lower inhibition observed in AD cerebral cortex.

The PET results might be explained if AChE activity in pretreatment AD brain were reduced primarily by compensatory downregulation operating to maintain ACh.[14] This would diminish the inhibitory drug effect specifically in AD cerebral cortex. The existence of such a compensatory mechanism has yet to be confirmed, but the issue is important for further study. Evidence against it is our finding that AChE activity reduction in mild AD is no more severe than cholinergic terminal loss.[3]

Currently, no peripheral surrogate marker has a valid one-to-one relationship with regional AChE inhibition in the brain. Inhibition in different tissues is a consequence of specific pharmacokinetics and pharmacodynamics that determine the inhibitor drug's accessibility to regional AChE. Consequently, measurements of AChE inhibition in peripheral RBC membranes usually overestimate inhibition in brain.[15] Accordingly, the plateau of RBC enzyme inhibition (80–90%) found at higher plasma concentrations in donepezil trials[2] is not reliable evidence that only marginal increases in cerebral cortical inhibition remain to be provided.

It has been proposed that AChE inhibition therapy fails commonly in mild AD because (1) there really is no cholinergic deficit,[16] (2) cholinergic terminals are too massively depleted,[17] or (3) AChE is already markedly depressed.[17] None of these postulates are supported by in vivo mapping studies of cholinergic terminal density[11] and AChE activity[3] in AD cerebral cortex. Is inadequate inhibition a major barrier to therapeutic success? Unless current drug schedules already provide maximum AChE inhibition in AD cerebral cortex, there is promise that alternative drugs or dose schedules might do better and be more effective. Meanwhile, it is important to avoid assumptions that maximum inhibition is being tested in clinical trials, if it is not.

Supported in part by US Public Health Service grants RO1 NS 24896 and NIA P50 AG08671, and Department of Energy grant DE-FG02-87ER60561.

We thank the PET chemistry staff for preparing [^{11}C]PMP, the technologist staff for data acquisition, Jill M. Rothley, BS, CNMT, and Donna Cross, BSE, for data workup and analysis; Kristine A. Wernette, RN, MS, and the nurses and staff of the Clinical Core of the Michigan Alzheimer's Disease Research Center for subject recruitment; Nancy R. Barbas, MD, and R. Scott Turner, MD, for referring their patients; and Olga L. Mancik and Karen M. Kreutzer for typing the manuscript.

References

1. Francis PT, Palmer AM, Snape M, Wilcock GK. The cholinergic hypothesis of Alzheimer's disease: a review of progress. J Neurol Neurosurg Psychiatry 1999;66:137–147
2. Rogers SL, Farlow MR, Doody RS, et al. A 24-week, double-

blind, placebo-controlled trial of donepezil in patients with Alzheimer's disease. Neurology 1998;50:136–145
3. Kuhl DE, Koeppe RA, Minoshima S, et al. In vivo mapping of cerebral acetylcholinesterase activity in aging and Alzheimer's disease. Neurology 1999;52:691–699
4. McKhann G, Drachman D, Folstein M, et al. Clinical diagnosis of Alzheimer's disease: report of the NINCDS-ADRDA Work Group under the auspices of Department of Health and Human Services Task Force on Alzheimer's disease. Neurology 1984;34:939–944
5. Hughes CP, Berg L, Danziger WL, et al. A new clinical scale for the staging of dementia. Br J Psychiatry 1982;140:566–572
6. Folstein M, Folstein SE, McHugh PR. "Mini Mental State": a practical method for grading the cognitive state of patients for the clinician. J Psychiatr Res 1975;12:189–198
7. Snyder SE, Tluczek L, Jewett DM, et al. Synthesis of 1-[^{11}C]methylpiperidin-4-yl propionate ([^{11}C]PMP) for in vivo measurements of acetylcholinesterase activity. Nucl Med Biol 1998;25:751–754
8. Minoshima S, Frey KA, Koeppe RA, et al. A diagnostic approach in Alzheimer's disease using three-dimensional stereotactic surface projections of [^{18}F]FDG. J Nucl Med 1995;36: 1238–1248
9. Gilmor ML, Erickson JD, Varoqui H, et al. Preservation of nucleus basalis neurons containing choline acetyltransferase and the vesicular acetylcholine transporter in the elderly with mild cognitive impairment and early Alzheimer's disease. J Comp Neurol 1999;411:693–704
10. Reinikainen KJ, Soininen H, Riekkinen PJ. Neurotransmitter changes in Alzheimer's disease: implications to diagnostics and therapy. J Neurosci Res 1990;27:576–586
11. Kuhl DE, Minoshima S, Fessler JA, et al. In vivo imaging of cholinergic terminals in normal aging, Alzheimer's disease and Parkinson's disease. Ann Neurol 1996;40:399–410
12. Irie T, Fukushi K, Akimoto Y, et al. Design and evaluation of radioactive acetylcholine analogs for mapping brain acetylcholinesterase (AchE) in vivo. Nucl Med Biol 1994;21:801–808
13. Perry EK, Perry RH, Blessed G, Tomlinson BE. Changes in brain cholinesterase in senile dementia of Alzheimer type. Neuropathol Appl Neurobiol 1978;4:273–277
14. DeKosky ST, Haybaugh RE, Schmitt FA, et al. Cortical biopsy in Alzheimer's disease: diagnostic accuracy and neurochemical, neuropathological, and cognitive correlations. Ann Neurol 1992;32:625–632
15. Lotti M. Cholinesterase inhibition: complexities in interpretation. Clin Chem 1995;41/12:1814–1818
16. Davis KL, Mohs RC, Marin D, et al. Cholinergic markers in elderly patients with early signs of Alzheimer disease. JAMA 1999;281:1401–1406
17. Ladner CJ, Lee JM. Pharmacological drug treatment of Alzheimer disease: the cholinergic hypothesis revisited. J Neuropath Exp Neurol 1998;57:719–731

An Enzyme-Linked Immunosorbent Assay to Quantify 14-3-3 Proteins in the Cerebrospinal Fluid of Suspected Creutzfeldt-Jakob Disease Patients

K. Kenney, MD,* C. Brechtel,* H. Takahashi, MD,†
K. Kurohara, MD,* Pat Anderson,*
and C. J. Gibbs, Jr, PhD*

The detection of 14-3-3 protein by Western immunoblot is a sensitive and specific cerebrospinal fluid marker of Creutzfeldt-Jakob disease (CJD). We developed a quantitative enzyme-linked immunosorbent assay (ELISA) that reliably detects 14-3-3 in cerebrospinal fluid. In a prospective study of 147 cerebrospinal fluid samples, the mean 14-3-3 concentration among pathologically confirmed CJD patients (28.0 ± 20.6 ng/ml, n = 41) is significantly higher than the mean in the cerebrospinal fluid of those with other neurological disorders (3.1 ± 2.9 ng/ml, n = 84). At a cutoff value of 8.3 ng/ml, the ELISA has a sensitivity of 92.7% and a specificity of 97.6%. The 14-3-3 ELISA supports a diagnosis of CJD in patients who fulfill clinical criteria for possible CJD.

Kenney K, Brechtel C, Takahashi H, Kurohara K, Anderson P, Gibbs CJ Jr. An enzyme-linked immunosorbent assay to quantify 14-3-3 proteins in the cerebrospinal fluid of suspected Creutzfeldt-Jakob disease patients. Ann Neurol 2000;48:395–398

Creutzfeldt-Jakob disease (CJD) was of little public notice until the emergence of new variant CJD (vCJD)[1] and evidence for a common etiological link between vCJD and bovine spongiform encephalopathy.[2,3] The possibility of an epidemic of vCJD has reinforced the need for noninvasive, rapid, and reliable tests in the diagnosis of CJD. The sensitivity and specificity of several noninvasive tests have been assessed[4–9] and international clinical diagnostic criteria have been estab-

From the *Laboratory of Central Nervous System Studies, National Institute of Neurological Disorders and Stroke, National Institutes of Health, Bethesda, MD, and †Department of Pathology, National Institute of Infectious Diseases, Tokyo, Japan.

Received Dec 10, 1999, and in revised form Apr 11, 2000. Accepted for publication May 11, 2000.

Address correspondence to Dr Gibbs, Chief, LCNSS, BNP, DIR, NINDS, NIH, Building 36, Room 4A-05, MSC 4122, 9000 Rockville Pike, Bethesda, MD 20892-4122.

lished.[10] Since we reported that the detection of cerebrospinal fluid (CSF) 14-3-3 protein is a sensitive and specific marker for CJD,[11] the 14-3-3 Western blot (WB) immunoassay's sensitivity and specificity has been corroborated by other laboratories[12] and is now routinely used worldwide. In 1998, the World Health Organization recommended that the clinical diagnostic criteria for probable CJD be amended to include either the detection of 14-3-3 protein in CSF or the diagnostic electroencephalogram.[13] Unfortunately, the WB assay is not informative regarding the magnitude of the 14-3-3 proteins or the relative contributions of the different 14-3-3 isoenzymes during the different stages of disease. Here we present a quantitative 14-3-3 ELISA, its validation, sensitivity, and specificity, and a comparison with the WB immunoassay.

Materials and Methods

Materials

14-3-3 protein was prepared from normal bovine brain[14] by Dr Paul Wagner (National Cancer Institute, National Institutes of Health, Bethesda, MD) and provided to us. Monoclonal anti–14-3-3 antibody (produced by immunization with recombinant 14-3-3b antigen) was provided by Dr Hidehiro Takahashi (Department of Pathology, National Institute of Infectious Diseases, Tokyo, Japan).

14-3-3 Antigen Capture Assay

We developed and optimized an indirect double sandwich ELISA as follows: Monoclonal capture anti–14-3-3 antibody was pipetted into each well of a microplate (NUNC Immuno Maxisorp FB, Roskilde, Denmark), and the plate was incubated overnight. Bovine 14-3-3 protein standards, ranging from 2.1 to 135.0 ng/ml, were prepared daily from a frozen stock solution in serial two-fold dilutions. Each well was loaded with 14-3-3 standard, diluent, or CSF test sample, and the microplate was incubated at 37°C. The plate was washed three times and blocked with a solution of BSA, sucrose, and nonfat dry milk. The detector antibody, rabbit anti–14-3-3b polyclonal antibody (Santa Cruz Biotechnology, Santa Cruz, CA), was loaded into each well, and the microplate was incubated for 1.5 hours. After washing, peroxidase-labeled goat anti-rabbit IgG antibody (KPL, Gaithersburg, MD) was loaded into each well, and the microplate was incubated at 37°C. TMB was added for colorimetric detection. The enzymatic reaction was stopped, and absorbance values were measured. Each CSF sample was run in duplicate in a blinded fashion. A control series of standard 14-3-3 antigen and diluent was included on every microplate.

14-3-3 Western Blot Method

We performed the WB as previously described by Hsich and associates[16] or by a modified protocol to incorporate precast gels. Molecular weight markers and CSF controls (from confirmed CJD and non-CJD patients) were included on every gel.

CSF Samples and CJD Diagnostic Criteria

CSF samples were prospectively collected from patients suspected of having CJD. Each patient with suspected CJD was assigned to one of four clinical diagnostic categories—definite CJD, probable CJD, possible CJD, or other neurological disorder (OND)—according to accepted criteria.[10] Follow-up clinical and pathological information was sought by questionnaire on each patient every 3 to 6 months. All CSF samples were kept frozen.

Of the 84 CSFs in the OND category in this study, 53 did not fulfill clinical criteria for possible CJD at initial presentation and were assigned to OND; of these, most had either a long-standing pure dementia or an acute reversible encephalopathy. Thirty-one specimens were from patients who initially fulfilled clinical criteria for possible CJD but who on subsequent testing or clinical follow-up were diagnosed with conditions other than CJD. These diagnoses are listed in Table 1.

Precision and Statistical Evaluation

Intra-assay precision was calculated by determining 14 sets of 14-3-3 standards simultaneously. Inter-assay precision was calculated by determining the same range of standards on consecutive days. The unpaired Student's t test was used to compare mean CSF 14-3-3 concentrations in two instances, definite CJD versus OND and definite plus probable CJD versus OND. In all cases, p values less than 0.05 were considered to be statistically significant. Confidence intervals were calculated by the exact method for a binomial parameter.

Results

Standardization of ELISA

A standard curve is linear for 14-3-3 concentrations ranging from 2.1 to 135 ng/ml with a correlation co-

Table 1. Alternate Diagnoses in Patients Suspected of CJD[a]

Diagnosis	No.
Encephalopathy	5
Encephalitis	4
CNS vasculitis	2
Meningitis	2
Neurosyphilis	2
Motor neuron disease	2
Multi-infarct dementia	2
Subacute ataxia	2
Alzheimer's	1
Alzheimer's + Lewy bodies	1
Glioblastoma multiforme	1
Glioma, temporal lobe	1
Gliosis	1
Leukoencephalopathy	1
Myoclonic epilepsy	1
Normal brain	1
Non-CJD pathology	1
Status epilepticus	1

[a]These patients initially fulfilled criteria for possible CJD, but were ultimately diagnosed with conditions other than CJD.

CJD = Creutzfeldt-Jakob disease.

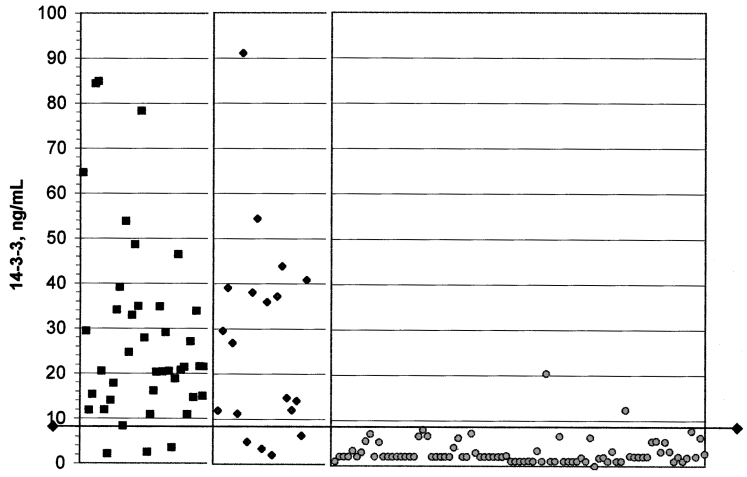

Fig. CSF 14-3-3 levels in patients stratified by CJD diagnosis category. The squares represent CSF 14-3-3 by ELISA in patients with definite CJD (n = 41); diamonds, CSF 14-3-3 analyses in patients with probable CJD (n = 19; 3 probable patients' levels are not shown because their levels were greater than 100 ng/ml); and the circles represent CSF 14-3-3 levels in patients with OND (n = 84). The horizontal line just below 10 corresponds to a 14-3-3 level of 8.3 ng/ml for reference.

efficient (R^2) of 1.00. The minimum detectable 14-3-3 concentration is 2.1 ng/ml (determined by adding 2 SD to the mean background value). The intra-assay and interassay coefficients of variation (CV) for standards in the 2.1- to 135-ng/ml working range are 0.03 are 0.10, respectively. Storage of the CSF at room temperature for up to 24 hours, and in one case for 6 days, did not significantly degrade the signal (data not shown). Thus, specimens may be sent to laboratories at room temperature by overnight mail and frozen at the testing laboratory site.

Diagnostic Application

There was a significant increase ($p < 0.0001$, Student's t test) in mean 14-3-3 CSF levels between definite CJD patients (28.0 ± 20.6 ng/ml) and OND (3.1 ± 2.9 ng/ml), as well as a significant increase ($p < 0.0001$, Student's t test) between probable CJD patients (56.4 ± 84.0 ng/ml) and OND (Fig). Combined definite and probable CJD had a mean 14-3-3 CSF level of 38.1 ± 53.0 ng/ml ($p < 0.0001$, Student's t test). With a 14-3-3 cutoff value of 8.3 ng/ml and considering definite CJD versus OND, the ELISA has a sensitivity of 92.7% and a specificity of 97.6%. The positive and negative predictive values are 95% and 96.5%, respectively. The WB has a sensitivity of 95.1% and specificity of 97.6% on the same specimen cohort. Combining both definite and probable CJD versus OND specimens, the ELISA has a sensitivity of 88.9% and the WB of 93.7%. Table 2 compares the statistical accuracy of the 14-3-3 ELISA with that of the 14-3-3 WB in these patient specimens.

Table 2. Detection of 14-3-3 Protein in Cerebrospinal Fluid in Patients with CJD and Other Neurological Disorders

	ELISA[a] (%)	Western Blot (%)
CJD	56/63 (88.9)	59/63 (93.7)
Definite	38/41 (92.7)	39/41 (95.1)
Probable	18/22 (81.8)	20/22 (90.9)
Other neurological disorder	2/84 (02.4)	2/84 (2.4)
Sensitivity (definite CJD)	(92.7)	(95.1)
Sensitivity (definite + probable CJD)	(88.9)	(93.7)
Specificity	(97.6)	(97.6)

[a]Using a selected cutoff of over 8.3 ng/ml.

CJD = Creutzfeldt-Jakob disease.

Discussion

We have developed a sensitive and precise ELISA for the quantification of 14-3-3 protein in CSF. The ELISA analysis of CSF from patients stratified by diagnosis category indicates a significantly higher 14-3-3 concentration in definite and probable CJD patients than in the CSF of patients with other neurological disorders.

The ELISA had three false-negative results among specimens from definite (14-3-3 values of 2.1, 2.5, 3.5 ng/ml) and four among probable CJD patients (14-3-3 values of 3.5, 2.1, 6.4, 5.0 ng/ml), whereas the WB had two each within the same specimen groups (these four were negative by both tests), for a total of seven versus four false-negatives. The three ELISA false-negatives that were positive by WB had values of 2.1, 3.5 and 5.0 ng/ml. The ELISA had two false-positive results: a patient each with CNS vasculitis (20.4 ng/ml) and temporal lobe glioma (12.4 ng/ml). The WB assay also had two false-positives: a patient each with aseptic meningitis (5.4 ng/ml) and status epilepticus (6.3 ng/ml). We do not know why there were differences among both the false-positive and false-negative groups by the two assays. It could be explained by the differences in antibody sensitivities, particularly because the monoclonal antibody used in the ELISA detects different 14-3-3 isoforms from the polyclonal antibody used

in the WB assay. The specimens in this study were restricted to those submitted prospectively to our laboratory by referring physicians considering the diagnosis of CJD in their patients. The numbers overall are limited, and more accurate sensitivity and specificity determinations will be made as more specimens are tested.

There are clear advantages to using the ELISA over the WB method for the detection of CSF 14-3-3 protein. Its quantitative nature yields greater information in longitudinal studies of experimentally induced TSEs. It tells us about the magnitude and duration of the proteins' presence. Further, ELISA obviates some of the inconsistencies inherent in the WB protocol. Variations in the number, location, and intensity of banding patterns can confound the assessment of the WB. Finally, the ELISA method facilitates the simultaneous processing of numerous CSF samples and is readily adaptable to a clinical laboratory setting.

In this study, an ELISA that quantifies 14-3-3 protein in CSF was developed. The method was validated in CSF samples from patients suspected of having CJD. A statistically significant increase was shown in CSF 14-3-3 level of patients with definite and probable CJD versus OND. When appropriately applied to patients fulfilling clinical criteria for possible CJD, the ELISA has a high sensitivity and specificity and supports a clinical diagnosis of CJD.

References

1. Will RG, Ironside JW, Zeidler M, et al. A new variant of Creutzfeldt-Jakob disease in the UK. Lancet 1996;347:921–925
2. Collinge J, Sidle KC, Meads J, et al. Molecular analysis of prion strain variation and the aetiology of "new variant" CJD. Nature 1996;383:685–690
3. Bruce ME, Will RG, Ironside JW, et al. Transmission to mice indicate that "new variant" CJD is caused by the BSE agent. Nature 1997;389:498–501
4. Finkenstaedt M, Szudra A, Zerr I, et al. Magnetic resonance imaging of Creutzfeldt-Jakob disease. Radiology 1996;199:793–798
5. Zerr I, Bodemer M, Räcker S, et al. Cerebrospinal fluid concentration of neuron-specific enolase in diagnosis of Creutzfeldt-Jakob disease. Lancet 1995;345:1609–1610
6. Otto M, Stein H, Szudra A, et al. Elevated level of S-100 protein concentration in CSF of patients with Creutzfeldt-Jakob disease. Akt Neurol 1996;23:71 (Abstract)
7. Otto M, Wiltfang J, Tumani H, et al. Elevated levels of tauprotein in CSF of patients with Creutzfeldt-Jakob disease. Neurosci Lett 1997;225:210–212
8. Jimi T, Wakayama Y, Shibuya S, et al. High levels of nervous system–specific proteins in cerebrospinal fluid in patients with early stage Creutzfeldt-Jakob disease. Clin Chim Acta 1992; 211:37–46
9. Manaka H, Kato T, Kurita K, et al. Marked increase in cerebrospinal fluid ubiquitin in Creutzfeldt-Jakob disease. Neurosci Lett 1992;139:47–49
10. Kretzschmar HA, Ironside JW, DeArmond SJ, Tateishi J. Diagnostic criteria for sporadic Creutzfeldt-Jakob disease. Arch Neurol 1996;53:913–920
11. Hsich G, Kenney K, Gibbs CJ, et al. The 14-3-3 brain protein in cerebrospinal fluid as a marker for transmissible spongiform encephalopathies. N Engl J Med 1996;335:924–930
12. Zerr I, Bodemer M, Gefeller O, et al. Detection of 14-3-3 protein in the cerebrospinal fluid supports the diagnosis of Creutzfeldt-Jakob disease. Ann Neurol 1998;43:32–40
13. Report of a WHO consultation. Global surveillance, diagnosis and therapy of human transmissible spongiform encephalopathies. World Health Organization, Geneva, Switzerland, 1998. WHO/EMC/ZDI/98.9
14. Ichimura T, Isobe T, Okuyama T et al. Brain 14-3-3 protein is an activator protein that activates tryptophan 5-monooxygenase and tyrosine 3-monooxygenase in the presence of Ca^{2+}, calmodulin-dependent protein kinase II. FEBS Lett 1987;219: 79–82

Correction

In the article by Leone et al (2000;48:27–38) in the July issue of *Annals of Neurology*, there were several errors:

1. In the list of authors: The correct spelling of the third author's name is L. **Bilaniuk**, MD, and Andrew Freese's degrees are MD, **PhD**.
2. On page 34, right column, last paragraph: The third sentence should read "At baseline, the T1 signal showed an abnormal prolongation within the subcortical and deep white matter, and the **T2-weighted images** showed a reciprocal abnormal signal (hyperintensity) that was particularly evident on FLAIR."
3. On page 36, left column: The first line should read ". . . tensity on **T1-weighted images**, suggesting new myelination of the cor- . . ."
4. Also on page 36, left column, first paragraph: The second full sentence should read "**T2-weighted images** at this time continued to show an abnormal hyperintensity consistent with spongiform pathology but with little interval change over the entire year after delivery."